Annu. Rev. Nucl. Part. Sci. 1999. 49:77–123

THE COSMIC MICROWAVE BACKGROUND AND PARTICLE PHYSICS

Marc Kamionkowski
Department of Physics, Columbia University, 538 West 120th Street, New York, New York 10027; e-mail: kamion@phys.columbia.edu

Arthur Kosowsky
Department of Physics and Astronomy, Rutgers University, Piscataway, New Jersey 08854-8019; e-mail: kosowsky@physics.rutgers.edu

Key Words cosmology, particle physics

■ **Abstract** In forthcoming years, connections between cosmology and particle physics will become increasingly important with the advent of a new generation of cosmic microwave background (CMB) experiments. Here, we review a number of these links. Our primary focus is on new CMB tests of inflation. We explain how the inflationary predictions for the geometry of the Universe and primordial density perturbations will be tested by CMB temperature fluctuations, and how the gravitational waves predicted by inflation can be pursued with the CMB polarization. The CMB signatures of topological defects and primordial magnetic fields from cosmological phase transitions are also discussed. Furthermore, we review current and future CMB constraints on various types of dark matter (e.g. massive neutrinos, weakly interacting massive particles, axions, vacuum energy), decaying particles, the baryon asymmetry of the Universe, ultra-high-energy cosmic rays, exotic cosmological topologies, and other new physics.

CONTENTS

0163-8998/99/1201-0077$08.00

1. OVERVIEW OF THE COSMIC MICROWAVE BACKGROUND

In 1948, Alpher & Hermann (1) realized that if light elements were produced in a hot big bang, as Gamow and others had suggested (2), then the Universe today should have a temperature of about 5 K. When Penzias & Wilson discovered an anomalous background in 1964, consistent with a blackbody spectrum at a temperature of $\sim$3 K (3), Dicke and his collaborators immediately recognized it as the radiation associated with this nonzero cosmological temperature (4). Subsequent observations that confirm a remarkable degree of isotropy [apart from a dipole (5, 6), which can be interpreted as our motion of $627 \pm 22\,\mathrm{km\,s^{-1}}$ with respect to the blackbody rest frame (7–10)] suggest an extragalactic origin for this cosmic microwave background (CMB). Strong upper limits to any angular cross-correlation between the CMB temperature and the extragalactic X-ray background intensity (11, 12) suggest that the CMB comes from redshifts greater than those probed by the active galactic nuclei and galaxy clusters ($z \simeq 2-4$) that produce the X-ray background. This evidence, as well as the exquisite blackbody spectrum of the CMB (13–15), further supports the notion that this radiation is the cosmological blackbody postulated by Alpher & Hermann.

Although they have a Planck spectrum, CMB photons are not in thermal equilibrium. The mean free path for scattering of photons in the Universe must be huge, or else we would not see galaxies and quasars out to distances of thousands of Mpc.[1] So where did these photons come from? At early times ($t \lesssim 10^5$ y; redshifts $z \gtrsim 1000$), the temperature of the Universe exceeded 1 eV, so the Universe consisted of a plasma of free electrons and light nuclei. CMB photons were tightly coupled to this plasma via Thomson scattering from the free electrons. At a redshift of $z \simeq 1000$, the temperature dropped below a few eV, and electrons and nuclei combined to form atoms. At this point, photons ceased interacting. A detailed analysis of "recombination" and the almost simultaneous (although slightly later) decoupling of photons shows that CMB photons last scattered near a redshift of $z \simeq 1100$ (16–18).

When we look at these CMB photons coming to us from all directions in the sky, we are therefore looking directly at a spherical surface in the Universe that surrounds us at a distance of $\sim 10^4$ Mpc, as it was when the Universe was only about 300,000 years old. The temperature of the CMB is found to be the same, to roughly one part in 10^5, in every direction in the sky. This remarkable isotropy poses a fundamental conundrum for the standard big bang theory. When these photons last scattered, the size of a causally connected region of the Universe was roughly 300,000 light years, and such a region subtends an angle of only one degree in the sky. Thus, when we look at the CMB, we are looking at roughly 40,000 causally disconnected regions of the Universe. How is it, then, that each of these has the same temperature to one part in 10^5? This is the well-known isotropy, homogeneity, or horizon problem.

Another fundamental question in cosmology today is the origin of the large-scale structure of the galaxy distribution. The simplest and most plausible explanation is that the observed mass inhomogeneities grew from tiny density perturbations in the early Universe via gravitational instability. Mass from underdense regions is drawn towards overdense regions, and in this way, small primordial perturbations are amplified into the structure we see in the Universe today. New support for this hypothesis was provided by the Cosmic Background Explorer (*COBE*) detection of temperature differences in the CMB of roughly one part in 10^5 (19). Heuristically, density perturbations induce gravitational-potential perturbations at the surface of last scatter; photons that arrive from denser regions climb out of deeper potential wells and thus appear redder than those from underdense regions [the Sachs-Wolfe effect (20)]. Thus, the temperature fluctuations seen with *COBE* provide a snapshot of the tiny primordial perturbations that gave rise to the large-scale structure we see in the Universe today. But this raises a second question: If large-scale structure grew via gravitational infall from tiny inhomogeneities in the early Universe, where did these primordial perturbations come from?

Before *COBE*, there was no shortage of ideas for the origin of large-scale structure, and—quite remarkably—all causal mechanisms for producing primordial

[1]Mpc $= 3.3 \times 10^6$ light years $= 3.09 \times 10^{24}$ cm.

perturbations have come from new ideas in particle theory: primordial adiabatic perturbations from inflation (21–25), late-time phase transitions (26, 27), a loitering Universe (28), scalar-field ordering (29, 30), topological defects (31, 32) [such as cosmic strings (33–36), domain walls (27, 37), textures (38, 39), or global monopoles (40, 41)], superconducting cosmic strings (42, 43), isocurvature axion perturbations (44–50), etc.

However, after *COBE*, primordial adiabatic perturbations (perturbations to the total density with equal fractional number-density perturbations in each species in the Universe) seem to provide the only workable models. Such perturbations are produced naturally during inflation, a period of exponential expansion in the early Universe driven by the vacuum energy associated with some new scalar field (57–59). With adiabatic perturbations, hotter regions at the surface of last scatter are embedded in deeper potential wells, so the reddening due to the gravitational redshift of the photons from these regions partially cancels the higher intrinsic temperatures. When normalized to the amplitude of density perturbations indicated by galaxy surveys, alternative models generically produce a larger temperature fluctuation than that measured by *COBE* (51–53). Recently, more detailed calculations of the expected CMB-anisotropy amplitude have led proponents of topological defects, the primary alternative to inflation, to concede that these models have difficulty accounting for the origin of large-scale structure (54–56).

Although inflation now seems to provide the best candidate for the origin of large-scale structure, the primary attraction of inflation was originally that it provided (and still provides) the best, if not only, solution of the horizon problem. For these reasons, inflation has taken center stage in cosmology. Although inflation was for a long time speculative physics beyond the realm of experimental tests, we are now entering a new era in which the predictions of inflation will be tested with unprecedented precision by CMB measurements.

The primary focus of this article is therefore to review the predictions of inflation and how they will be tested with the CMB. Although inflation currently seems to provide the most promising paradigm for the origin of large-scale structure, it is not yet well established. Moreover, although the simplest topological-defect models seem to be ruled out, it is still certainly plausible that some more involved models may be able to account for large-scale structure. We therefore review the CMB predictions of topological-defect models. We also discuss a number of other promising links between the CMB and particle physics that do not necessarily have to do with the origin of structure, e.g. dark matter, neutrino properties, decaying particles, cosmological magnetic fields from early-Universe phase transitions, parity violation, gravity theories, time variation of fundamental parameters, and baryogenesis scenarios.

We are unfortunately unable to cover the larger bodies of excellent work on the CMB in general, nor on the intersections between particle physics and cosmology more generally. Fortunately, a number of excellent reviews cover those subjects, to which we cannot do justice here. Lyth & Riotto (60) review particle-physics models of inflation; Liddle & Lyth (61) discuss structure formation in inflation-inspired

cold-dark-matter models. Lidsey et al (62) review the production of density perturbations and reconstruction of the inflaton potential from the power spectra of density perturbations and gravitational waves. White et al (63) review the CMB and structure formation, and Hu & White (64) provide a brief review of the theory of CMB polarization. Finally, see References 65–67 for reviews of the Sunyaev-Zeldovich effect (the scattering of CMB photons from hot gas in clusters of galaxies), an intriguing and potentially very important probe of the physics of clusters.

2. COSMIC MICROWAVE BACKGROUND OBSERVABLES

2.1 The Frequency Spectrum

Standard cosmology predicts the CMB frequency spectrum to be that of a perfect blackbody,

$$S(\nu; T) = \frac{2hc^2\nu^3}{e^x - 1}, \qquad 1.$$

where $x = hc\nu/kT$, h is Planck's constant, c is the velocity of light, ν is the frequency, k is Boltzmann's constant, and T is the temperature. Of the infinitude of possible distortions to this spectrum, two forms often considered in the literature—Bose-Einstein and Compton distortions—could arise from physical processes before recombination.

If photons are released into the Universe from some nonthermal process (e.g. decay of a massive particle) when the temperature of the Universe exceeds roughly 1 keV (redshifts $z \gtrsim 10^6$ when the age of the Universe is $t \lesssim 10^7$ sec), they will come into complete thermal equilibrium with the photons in the primordial plasma. More precisely, they attain kinetic equilibrium through Compton scattering, double Compton scattering, and bremsstrahlung, and they attain chemical equilibrium (chemical potential $\mu = 0$) because the rate for photon-number-changing processes (e.g. $\gamma\gamma \rightarrow \gamma\gamma\gamma$) that maintain a chemical potential $\mu = 0$ exceeds the expansion rate. Therefore, if any electromagnetic energy is released into the Universe at such early times, it will have no observable effect on the CMB. However, if photons are released at later times (but still before recombination), they can distort the CMB frequency spectrum (65, 68–75).

2.1.1 Bose-Einstein Distortion

Nonthermal photons produced in the redshift range $10^5 \lesssim z \lesssim 3 \times 10^6$ (temperatures $T \simeq 0.1 - 1$ keV and ages $t \simeq 10^{7-9}$ sec) can still attain kinetic equilibrium, but they will not attain chemical equilibrium, as interactions that change the photon number occur less rapidly than the expansion rate. If electromagnetic energy is released at these times, the CMB frequency dependence will be that of a

Bose-Einstein gas with a nonzero chemical potential,

$$S(\nu; T, \mu) = \frac{2hc^2\nu^3}{e^{x+\mu} - 1}, \qquad 2.$$

where μ is the (dimensionless) chemical potential. The Far Infrared Absolute Spectrophotometer (FIRAS) result is $\mu = (-1 \pm 10) \times 10^{-5}$ or a 95% confidence-level upper limit of $|\mu| < 9 \times 10^{-5}$ (15). It is possible that values of μ as small as 10^{-6} could be probed by a future satellite mission (76).

2.1.2 Compton Distortion

If photons are released at later times ($z \lesssim 10^5$) but still before recombination ($z \simeq 1100$; temperatures $T \simeq 1 - 100$ eV and times $t \simeq 10^{9-13}$ sec), they do not have enough time to come to either thermal or kinetic equilibrium and wind up producing a "Compton distortion" of the form

$$S(\nu; T, y) = \frac{2hc^2\nu^3}{e^x - 1}\left(1 + yx\frac{1}{1 - e^{-x}}\,[x\,\coth(x/2) - 4]\right), \qquad 3.$$

to linear order in y (the Kompaneets or "Compton-y" parameter). If some CMB photons were rescattered after recombination by a hot intergalactic gas, this would also produce a Compton-y distortion. The FIRAS result for this type of distortion is $y = -1 \pm 6 \times 10^{-6}$ or an upper limit of $|y| < 15 \times 10^{-6}$ at the 95% confidence level (15). The consensus among the experimentalists we have surveyed seems to be that it would be difficult to improve on this limit.

2.2 Temperature and Polarization Power Spectra

The primary aim of forthcoming CMB satellite experiments, such as NASA's Microwave Anisotropy Probe (MAP) (77) and the European Space Agency's Planck Surveyor (78), will be to map the temperature $T(\hat{\mathbf{n}})$ of the CMB and its linear polarization, described by Stokes parameters $Q(\hat{\mathbf{n}})$ and $U(\hat{\mathbf{n}})$, as functions of position $\hat{\mathbf{n}}$ in the sky. Several temperature-polarization angular correlation functions, or equivalently, power spectra, can be extracted from such maps. These quantities can be compared with detailed predictions from cosmological models.

2.2.1 Harmonic Analysis for Temperature Anisotropies and Polarization

Temperature Anisotropies The temperature map can be expanded in spherical harmonics,

$$\frac{T(\hat{\mathbf{n}})}{T_0} = 1 + \sum_{lm} a^{\rm T}_{(lm)} Y_{(lm)}(\hat{\mathbf{n}}), \qquad 4.$$

where the mode amplitudes are given by

$$a^{\rm T}_{(lm)} = \frac{1}{T_0}\int d\hat{\mathbf{n}}\, T(\hat{\mathbf{n}})\, Y^*_{(lm)}(\hat{\mathbf{n}}); \qquad 5.$$

this follows from the orthonormality of the spherical harmonics. Here, $T_0 = 2.728 \pm 0.002$ K is the cosmological mean CMB temperature.

Linear Polarization The Stokes parameters (where Q and U are measured with respect to the polar $\hat{\theta}$ and azimuthal $\hat{\phi}$ axes) are components of a 2×2 symmetric traceless tensor with two independent components,

$$\mathcal{P}_{ab}(\hat{\mathbf{n}}) = \frac{1}{2}\begin{pmatrix} Q(\hat{\mathbf{n}}) & -U(\hat{\mathbf{n}})\sin\theta \\ -U(\hat{\mathbf{n}})\sin\theta & -Q(\hat{\mathbf{n}})\sin^2\theta \end{pmatrix}, \qquad 6.$$

where the subscripts ab are tensor indices, and Q and U are given in temperature units. Just as the temperature is expanded in terms of spherical harmonics, the polarization tensor can be expanded (79–82),

$$\frac{\mathcal{P}_{ab}(\hat{\mathbf{n}})}{T_0} = \sum_{lm} \left[a^{\mathrm{G}}_{(lm)} Y^{\mathrm{G}}_{(lm)ab}(\hat{\mathbf{n}}) + a^{\mathrm{C}}_{(lm)} Y^{\mathrm{C}}_{(lm)ab}(\hat{\mathbf{n}})\right], \qquad 7.$$

in terms of tensor spherical harmonics, $Y^{\mathrm{G}}_{(lm)ab}$ and $Y^{\mathrm{C}}_{(lm)ab}$. It is well known that a vector field can be decomposed into a curl (C) and a curl-free (gradient) (G) part. Similarly, a 2×2 symmetric traceless tensor field can be decomposed into a tensor analogue of a curl and a gradient part; the $Y^{\mathrm{G}}_{(lm)ab}$ and $Y^{\mathrm{C}}_{(lm)ab}$ form a complete orthonormal basis for the "gradient" (i.e. curl-free) and "curl" components of the ents of the tensor field, respectively.[2] Lengthy but digestible expressions for the $Y^{\mathrm{G}}_{(lm)ab}$ and $Y^{\mathrm{C}}_{(lm)ab}$ are given in terms of derivatives of spherical harmonics and also in terms of Legendre functions in Reference 80. The mode amplitudes in Equation 7 are given by

$$\begin{aligned} a^{\mathrm{G}}_{(lm)} &= \frac{1}{T_0}\int d\hat{\mathbf{n}}\, \mathcal{P}_{ab}(\hat{\mathbf{n}})\, Y^{\mathrm{G}\,ab\,*}_{(lm)}(\hat{\mathbf{n}}), \\ a^{\mathrm{C}}_{(lm)} &= \frac{1}{T_0}\int d\hat{\mathbf{n}}\, \mathcal{P}_{ab}(\hat{\mathbf{n}})\, Y^{\mathrm{C}\,ab\,*}_{(lm)}(\hat{\mathbf{n}}), \end{aligned} \qquad 8.$$

which can be derived from the orthonormality properties of these tensor harmonics (80). Thus, given a polarization map $\mathcal{P}_{ab}(\hat{\mathbf{n}})$, the G and C components can be isolated by first carrying out the transformations in Equation 8 to the $a^{\mathrm{G}}_{(lm)}$ and $a^{\mathrm{C}}_{(lm)}$ and then summing over the first term on the right-hand side of Equation 7 to get the G component and over the second term to get the C component.

2.2.2 The Power Spectra

Theories for the origin of large-scale structure predict that the mass distribution in the Universe is a single realization of a statistically isotropic random field. In other words, the Fourier components $\tilde{\delta}(\vec{k})$ of the fractional density perturbation $\delta(\vec{x}) = [\rho(\vec{x}) - \overline{\rho}]/\overline{\rho}$ [where $\rho(\vec{x})$ is the density at comoving position $\vec{x}$ and $\overline{\rho}$

[2]Our G and C are sometimes referred to as the scalar and pseudoscalar components (83), respectively, or with slightly different normalization as E and B modes (82).

is the universal mean density] are random variables that have expectation values $\langle\tilde{\delta}(\vec{k})\rangle = 0$ and covariance given by

$$\langle\tilde{\delta}(\vec{k})\tilde{\delta}(\vec{k}')\rangle = (2\pi)^3\,\delta_D(\vec{k}+\vec{k}')\,P_s(k). \qquad 9.$$

Here, $P_s(k)$ is the scalar power spectrum (so called because density perturbations produce scalar perturbations to the spacetime metric), or alternatively, the power spectrum for the spatial mass distribution. Statistical isotropy demands that the power spectrum depends only on the amplitude (rather than orientation) of $\vec{k}$.

Because the temperature perturbation and polarization of the CMB are due to density perturbations, the $a^{\rm X}_{(lm)}$ must be random variables with zero mean, $\langle a^{\rm X}_{(lm)}\rangle = 0$, and covariance,

$$\left\langle \left(a^{\rm X'}_{(l'm')}\right)^* a^{\rm X}_{(lm)} \right\rangle = C_l^{\rm XX'}\delta_{ll'}\delta_{mm'}, \qquad 10.$$

for $\rm X, X' = \{T, G, C\}$. The statistical independence of each lm mode (i.e. the presence of the Kronecker deltas) is a consequence of statistical isotropy. The scalar spherical harmonics $Y_{(lm)}$ and the gradient tensor spherical harmonics $Y^{\rm G}_{(lm)}$ have parity $(-1)^l$, whereas the curl tensor spherical harmonics $Y^{\rm C}_{(lm)}$ have the opposite parity, $(-1)^{l+1}$. Thus, $C_l^{\rm TC} = C_l^{\rm GC} = 0$ if the physics that gives rise to temperature anisotropies and polarization is parity-invariant. In this case, the two-point statistics of the CMB temperature-polarization map are completely specified by the four sets of moments, $C_l^{\rm TT}$, $C_l^{\rm TG}$, $C_l^{\rm GG}$, and $C_l^{\rm CC}$. Nonzero $C_l^{\rm TC}$ or $C_l^{\rm GC}$ would provide a signature of cosmological parity breaking.

2.2.3 Angular Correlation Functions

The temperature two-point correlation function is

$$C^{\rm TT}(\alpha) = \left\langle \frac{\Delta T(\hat{\mathbf{m}})}{T}\frac{\Delta T(\hat{\mathbf{n}})}{T}\right\rangle_{\hat{\mathbf{m}}\cdot\hat{\mathbf{n}}=\cos\alpha}, \qquad 11.$$

where the average is over all pairs of points in the sky separated by an angle α. It can be written in terms of the temperature power spectrum (i.e. the $C_l^{\rm TT}$) as

$$C^{\rm TT}(\alpha) = \sum_l \frac{2l+1}{4\pi} C_l^{\rm TT} P_l(\cos\alpha), \qquad 12.$$

where $P_l(\cos\alpha)$ are Legendre polynomials. Likewise, orthonormality of Legendre polynomials guarantees that the multipole coefficients, $C_l^{\rm TT}$, can be written as integrals over the product of the correlation function and a Legendre polynomial. Thus, specification of the correlation function is equivalent to specification of the power spectrum, and vice versa. CMB theorists and experimentalists have now adopted the convention of showing model predictions and presenting experimental results as power spectra (C_l) rather than as correlation functions, and we subsequently stick to this convention. Auto- and cross-correlation functions for the Stokes parameters and temperature-polarization cross-correlation functions

can also be defined and written in terms of the polarization and temperature-polarization power spectra (80), but we do not list them here.

In practice, the temperature intensity (or polarization) can never be determined at a given point in the sky; it can only be measured by a receiver of some finite angular resolution (referred to as a "finite beamwidth"). Thus, the correlation function in Equation 12 cannot be measured; one can only measure a smoothed version. Likewise, a finite beamwidth $\theta_{\rm fwhm}$ (at full-width half maximum) limits determination of the power spectrum to multipole moments $l \lesssim 200\,(\theta_{\rm fwhm}/1^\circ)^{-1}$.

The Differential Microwave Radiometer (DMR) experiment (8) aboard *COBE* produced the first map of the temperature of the CMB. The receivers also provided some information on the polarization, but the sensitivity was not sufficient to detect the signal expected in most cosmological models. Measurements of the CMB intensity were made at three different frequencies (31.5, 53, and 90 GHz) near the blackbody peak to disentangle the possible contribution of foreground contaminants (e.g. dust or synchrotron emission) from the Galaxy, as these would have a frequency spectrum that differs from a blackbody. The DMR beamwidth was 7°, so the temperature power spectrum was recoverable only for $l \lesssim 15$. MAP, scheduled for launch in the year 2000, will map the sky with an angular resolution better than 0.3° ($l \lesssim 700$). MAP should have sufficient sensitivity to see the polarization, although probably not enough to map the polarization power spectra precisely (the polarization is expected to be roughly an order of magnitude smaller than the temperature anisotropy). The Planck Surveyor, scheduled for launch around 2007, will map the temperature and polarization with even finer angular resolution (out to $l \lesssim 2000 - 3000$). Its sensitivity should be sufficient to map the polarization power spectra expected from density perturbations (discussed below) with good precision.

2.3 Gaussianity

Angular three-point and higher n-point temperature correlation functions can be constructed analogously to the two-point correlation functions in Equation 11. Fourier analogs of higher-order correlation functions can be defined. In particular, the temperature bispectrum $B(l_1, l_2, l_3)$ is the l-space version of the temperature three-point correlation function. It is defined by

$$\left\langle a^{\rm T}_{(l_1 m_1)} a^{\rm T}_{(l_2 m_2)} a^{\rm T}_{(l_3 m_3)} \right\rangle = \begin{pmatrix} l_1 & l_2 & l_3 \\ m_1 & m_2 & m_3 \end{pmatrix} B(l_1, l_2, l_3), \qquad 13.$$

where the array is the Wigner $3j$ symbol. This particular m and l dependence follows from the assumption of statistical isotropy. Closely related statistics include the skewness and kurtosis (respectively, the three- and four-point correlation functions at zero lag) (84–86) and higher cumulants (the higher n-point correlation functions at zero lag) (87). As discussed further below, inflationary models predict the primordial distribution of perturbations to be perfectly (or very nearly) Gaussian. Gaussianity dictates that all the odd-n n-point correlation functions vanish

and that for even n, the higher n-point correlation functions can be given in terms of the two-point correlation function.

Numerous other statistical tests of CMB Gaussianity have also been proposed, including (but not limited to) topology of temperature contours (88–90) and the related Minkowski functionals (91, 92), temperature peak statistics (90, 93, 94), Fourier space patterns (95, 96), and wavelet analysis (97, 98).

3. PREDICTIONS OF INFLATION

If the energy density of the Universe is dominated by matter or radiation, then the expansion of the Universe is decelerating. If so, the horizon grows more rapidly than the scale factor. In such a Universe, objects that are now beyond our horizon and therefore inaccessible to us will eventually enter the horizon and become visible. Thus, the observable Universe contains more information and is more complicated at later times. Inflation postulates the existence of a period of accelerated expansion in the early Universe. In such a Universe, the scale factor grows more rapidly than the horizon. Thus, objects currently visible to any given observer will eventually exit that observer's horizon (in much the same way that objects that fall into a black hole disappear when they pass through the black hole's event horizon). A period of accelerated expansion therefore makes the Universe simpler and smoother. As we now discuss, this accelerated expansion also generically drives the observable Universe to be flat and provides a mechanism for producing primordial density perturbations and gravitational waves.

3.1 Scalar-Field Dynamics

Inflation supposes the existence of some new scalar field ϕ (the "inflaton"), with a potential $V(\phi)$ that roughly resembles either of those shown in Figure 1. The shape is not particularly important. All we require is that, at some time in the history of the Universe, the field is displaced from the minimum of the potential, and then it rolls slowly. How slowly is slowly enough? This is determined by the

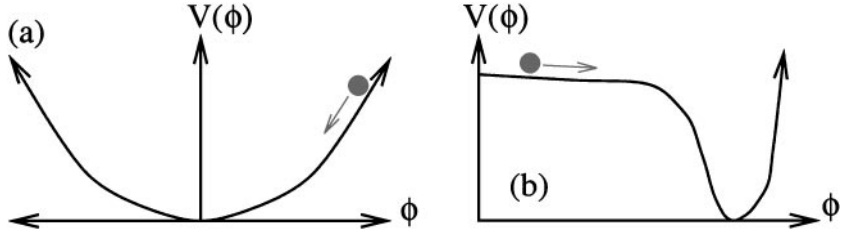

Figure 1 Two toy models for the inflationary potential.

Friedmann equation,

$$H^2 \equiv \left(\frac{\dot{a}}{a}\right)^2 = \frac{8\pi G\rho}{3} - \frac{k}{a^2} = \frac{8\pi G}{3}\left(\frac{1}{2}\dot{\phi}^2 + V(\phi)\right) - \frac{k}{a^2}, \qquad 14.$$

which governs the time t dependence of the scale factor $a(t)$ of the Universe (the dot denotes derivative with respect to time), as well as the scalar-field equation of motion,

$$\ddot{\phi} + 3H\dot{\phi} + V'(\phi) = 0, \qquad 15.$$

where $V' = dV/d\phi$. In Equation 14, ρ is the energy density of the Universe, which is assumed to be dominated by the inflaton potential-energy density $V(\phi)$ and kinetic-energy density $\dot{\phi}^2/2$. The term k/a^2 is the curvature term, and $k > 0$, $k < 0$, or $k = 0$ for a closed, open, or flat Universe, respectively. Note that the expansion acts as a friction term for the scalar-field equation of motion in Equation 15. If

$$\epsilon \equiv \frac{m_{\rm Pl}^2}{16\pi}\left(\frac{V'}{V}\right)^2 \ll 1, \qquad 16.$$

and

$$\eta \equiv \frac{m_{\rm Pl}^2}{8\pi}\left[\frac{V''}{V} - \frac{1}{2}\left(\frac{V'}{V}\right)^2\right] \ll 1, \qquad 17.$$

where $m_{\rm Pl} = 1.22 \times 10^{19}$ GeV is the Planck mass, then the field rolls slowly enough so that the requirement for acceleration [$p < -\rho/3$, where $p = (1/2)\dot{\phi}^2 - V$ is the pressure and $\rho = (1/2)\dot{\phi}^2 + V$ is the energy density] is satisfied. (Note that definitions of ϵ and especially of η may differ in some papers.)

The identity of the inflaton remains a mystery. It was originally hypothesized to be associated with a Higgs field in grand unified theories, but it may also have something to do with Peccei-Quinn symmetry breaking, a dilaton field, electroweak-symmetry breaking (99), some new pseudo-Nambu-Goldstone symmetry (100, 101), supersymmetry (102), or some other new physics. As discussed below, the primary predictions of slow-roll inflation do not depend on the details of the physics responsible for inflation but rather on some gross features that are easily quantified.

3.2 The Geometry

Given any inflationary potential $V(\phi)$, the equations of motion in Equations 14 and 15 can be solved numerically, if not analytically. Heuristically, during inflation, the potential $V(\phi)$ is roughly constant and $\dot{\phi}^2 \ll V(\phi)$. If the curvature term is appreciable initially, it rapidly decays relative to the potential term as the Universe expands, and the solution for the scale factor approaches an exponential,

$a(t) \propto e^{-Ht}$. If k is nonzero initially, the curvature term is then driven exponentially to zero during the inflationary epoch. In other words, if the duration of inflation is sufficiently long to place the observable Universe in a causally connected pre-inflationary patch, then the curvature radius is generically inflated to an exponentially (and unobservably) large value. In the language above, any initial nonzero curvature disappears beyond the horizon during accelerated expansion. Thus, the first prediction of slow-roll inflation is that the Universe should be flat today; i.e. the total density of all components of matter should sum to the critical density.

3.2.1 "Open Inflation"

It is, of course, mathematically possible that inflation did occur but that the inflationary epoch was prematurely terminated (103, 104) at just the right time so that the Universe today would be open with density $\Omega_0 \simeq 0.3$. Such a model requires some additional mechanism (e.g. another prior period of inflation and/or some arbitrary new "feature" in the inflaton potential) to solve the isotropy problem as well as to produce density perturbations. Several such open-inflation models have recently been constructed (103, 105–110), motivated by observations that suggest $\Omega_0 \simeq 0.3$. The predictions of a scale-invariant spectrum and Gaussian perturbations (discussed below) are the same as in ordinary inflation, but the Universe would be open. We do not find these models nearly as compelling as the ordinary slow-roll models that produce a flat Universe, although some theorists may disagree. Fortunately, the correct model will not be determined by debate; forthcoming CMB measurements, described below, should distinguish conclusively between these two classes—simple and elegant versus complicated and unappealing—of inflationary models.

3.3 Density Perturbations, Gravitational Waves, and the Inflationary Observables

3.3.1 Production of Density Perturbations

Density perturbations are produced as a result of novel quantum-mechanical effects (analogous to the production of Hawking radiation from black holes) that occur in a Universe with accelerating expansion (21–25). This process has been reviewed in detail recently (62, 111), so here we review the physics only heuristically. Consider perturbations $\delta\phi(\vec{x}, t)$ (as a function of comoving position $\vec{x}$) to the homogeneous slowly rolling field $\phi(t)$. These perturbations satisfy a massless Klein-Gordon equation, and the equation of motion for each Fourier mode $\widetilde{\delta\phi}(\vec{k})$ is that of a simple harmonic oscillator in an expanding Universe. At sufficiently early times, when the wavelength of any given Fourier mode is less than the Hubble radius H^{-1}, it undergoes quantum-mechanical zero-point oscillations. However, if the expansion is accelerating, then the physical wavelength of this comoving scale grows faster than the Hubble radius and eventually becomes larger than H^{-1}. At this point, crests and troughs of a given Fourier mode can no longer communicate,

and the zero-point fluctuation becomes frozen in as a classical perturbation $\delta\phi(\vec{x})$ to the scalar field. Because the inflaton potential is not perfectly flat, this induces perturbations to the density $\delta\rho(\vec{x}) = (\partial V/\partial\phi)\delta\phi(\vec{x})$.

3.3.2 Production of Gravitational Waves

Tensor perturbations to the spacetime metric (i.e. gravitational waves) satisfy a massless Klein-Gordon equation. A stochastic background of gravitational waves is therefore produced in the same way as classical perturbations to the inflaton are produced (112). Moreover, the power spectra for the inflaton-field perturbations and for the tensor metric perturbations should be identical. The power spectrum of density perturbations is a little different from that for gravitational waves because a density perturbation is related to a scalar-field perturbation by $\delta\rho = (\partial V/\partial\phi)\delta\phi$. The production of scalar and tensor perturbations depends only on the expansion rate during inflation. If the expansion rate were perfectly constant during inflation, it would produce flat scalar and tensor power spectra, $P_s \propto k$ [the "Peebles-Harrison-Zeldovich" (113–115) spectrum] and $P_t(k) \propto$ constant.

3.3.3 Inflationary Observables

A constant expansion rate is an oversimplification because the field must in fact be rolling slowly down the potential during inflation. Given any specific functional form for the potential, it is straightforward, using the tools of quantum field theory in curved spacetimes (see e.g. 116), to predict precisely the functional forms of $P_s(k)$ and $P_t(k)$. Measurement of these power spectra could then be used to reconstruct the inflaton potential (62). Since the field must be rolling fairly slowly during inflation, a good approximation (in most models) can be obtained by expanding about a constant expansion rate. In this slow-roll approximation, the primordial scalar power spectrum is[3]

$$P_s = A_s k^{n_s}, \qquad 18.$$

and the primordial power spectrum for tensor perturbations is

$$P_t = A_t k^{n_t}. \qquad 19.$$

The amplitudes A_t and A_s and power-law indices n_s and n_t have come to be known as the "inflationary observables." These parameters can provide information on the inflaton potential. In the slow-roll approximation, the power-spectrum indices are roughly constant and given by (62, 101, 117–127)

$$n_s = 1 - 4\epsilon + 2\eta, \quad n_t = -2\epsilon, \qquad 20.$$

[3]Note that this is the spectrum for the primordial perturbations. After the Universe becomes matter-dominated at a redshift $z \simeq 10^4$, density perturbations grow via gravitational infall, and the growth factor depends on the wave number. Therefore, the power spectrum for matter today is different from the primordial spectrum (it becomes k^{-4} times the primordial spectrum at large k), but it is straightforward to relate the primordial and current power spectra.

where ϵ and η are the slow-roll parameters given in Equations 16 and 17. Strictly speaking, ϵ and η may change (logarithmically with k) during inflation (62, 128), but, as the name implies, the field rolls slowly during slow-roll inflation, so the running of the spectral indices is, for all practical purposes, very small.

The amplitudes A_s and A_t are similarly fixed by the inflaton potential, but their precise values depend on Fourier conventions and on how the scale factor today is chosen. However, A_s and A_t are proportional, respectively, to the amplitudes of the scalar and tensor contributions to $C_2^{\rm TT}$, the quadrupole moment of the CMB temperature. In terms of the slow-roll parameter ϵ and height V of the inflaton potential during inflation, these CMB observables are

$$\begin{aligned} \mathcal{S} &\equiv 6\, C_2^{\rm TT,scalar} = 0.66\, \frac{V}{\epsilon m_{\rm Pl}^4} \\ \mathcal{T} &\equiv 6\, C_2^{\rm TT,tensor} = 9.2 \frac{V}{m_{\rm Pl}^4}. \end{aligned} \qquad 21.$$

For nearly scale-invariant spectra, *COBE* fixes $C_2^{\rm TT} = C_2^{\rm TT,scalar} + C_2^{\rm TT,tensor} = (1.0 \pm 0.1) \times 10^{-10}$. In terms of the slow-roll parameters, the tensor-to-scalar ratio is usually defined to be

$$r \equiv \frac{\mathcal{T}}{\mathcal{S}} = 13.7\, \epsilon. \qquad 22.$$

Comparing Equation 22 with Equation 20, we observe that the observables n_t and r satisfy a consistency relation, $n_t = -0.146\, r$, in slow-roll models.

To summarize, slow-roll inflation models (which account for the overwhelming majority of inflation models that appear in the literature) are parameterized by (*a*) the height V of the inflaton potential (i.e. the energy scale of inflation), (*b*) ϵ, which depends on the first derivative V' of the inflaton potential, and (*c*) η, which depends additionally on the second derivative V''.

The discussion above suggests that because the inflaton is always rolling down the potential, the scalar spectral index must be $n_s < 1$. Although this may be true for simple single-field inflation models, more complicated models (e.g. with multiple fields or with different potentials) may produce "blue" spectra with $n_s > 1$ (129).

COBE alone already constrains $V^{1/4} \leq 2.3 \times 10^{16}$ GeV. With some additional (but reasonable) modeling, the *COBE* constraint can be combined with current degree-scale CMB-anisotropy measurements and large-scale-structure observations to reduce this to $V^{1/4} \leq 1.7 \times 10^{16}$ GeV (e.g. 130). The *COBE* anisotropy implies $n_s = 1.1 \pm 0.3$ if it is attributed entirely to density perturbations (131), or $n_t = 0.2 \pm 0.3$ if it is attributed entirely to gravitational waves. Therefore, barring strange coincidences, the *COBE* spectral index and the relations above seem to suggest that if slow-roll inflation is right, then the scalar and tensor spectra must both be nearly scale-invariant ($n_s \simeq 1$ and $n_t \simeq 0$).

3.4 Character of Primordial Perturbations

3.4.1 Adiabatic Versus Isocurvature

The density perturbations produced by quantum fluctuations in the inflaton field are referred to as adiabatic, curvature, or isentropic perturbations. These are perturbations to the total density of the Universe, or equivalently, scalar perturbations to the spacetime metric. Adiabaticity further implies that the spatial distribution of each species in the Universe (e.g. baryons, photons, neutrinos, dark matter) is the same—that is, the ratio of number densities of any two of these species is everywhere the same.

Adiabatic perturbations can be contrasted with primordial isocurvature, or equivalently, pressure or entropy perturbations, which are perturbations to the ratios between the various species in the Universe (usually in a Universe with a homogeneous total density). Such varying ratios would set up perturbations to the pressure or equivalently to the entropy. When two initially causally-disconnected regions with different pressures come into causal contact, the pressure perturbations push matter around, thus seeding large-scale structure.

Axion Inflation Although adiabatic perturbations are generically produced during inflation, it is also possible to obtain isocurvature perturbations. One example is isocurvature perturbations to an axion density from quantum fluctuations in the Peccei-Quinn field during inflation (44–50). As discussed below, comparison of the measured amplitude of CMB anisotropies with the amplitude of galaxy clustering essentially rules out these models. Inflation models that produce both adiabatic and isocurvature perturbations have also been considered (132–142); future experiments should tightly constrain the relative contributions of the two types of perturbations.

3.4.2 Causal Versus Acausal

Perturbations produced by inflation are said to be super-horizon or acausal perturbations. This simply refers to the fact that inflation produces a primordial (meaning before matter-radiation equality, when gravitational amplification of perturbations can begin) spectrum of perturbations of all wavelengths, including those much larger than the Hubble length at any given time. This is to be contrasted, for example, with causal models of structure formation, in which perturbations are generated by causal physics on scales smaller than the horizon. Since inflation implies distance scales much larger than the Hubble length can be within a causally connected pre-inflationary patch, the term acausal is really a misnomer.

3.4.3 (Nearly) Gaussian Distribution of Perturbations

If the inflaton potential is flat enough for the slow-roll approximation to be valid, then each Fourier mode of the inflaton perturbation evolves independently; that

is, the inflaton behaves essentially like an uncoupled massless scalar field. As a result, inflation predicts that the primordial density field is a realization of a Gaussian random field: each Fourier mode is decoupled from every other, and the probability distribution for each is Gaussian.

Of course, Gaussianity is an approximation that becomes increasingly valid in the slow-roll limit, in which the inflaton perturbation can be treated as a noninteracting scalar field. Deviations from Gaussianity are generally accepted to be small, and most theorists have adopted a pure Gaussian distribution as a prediction of inflation. However, the deviations in some models might be observable and, if so, would shed light on the physics responsible for inflation (143–147).

This can be quantified more precisely with the three-point statistic (148),

$$I_l^3 \equiv \frac{1}{(2l+1)^{3/2}\left(C_l^{\rm TT}\right)^{3/2}} \begin{pmatrix} l & l & l \\ 0 & 0 & 0 \end{pmatrix} B(l,l,l). \qquad 23.$$

In slow-roll models with smooth inflaton potentials, the prediction for this quantity is (L Wang, M Kamionkowski, manuscript in preparation)

$$\sqrt{l(l+1)}I_l^3 = \frac{2}{m_{\rm Pl}^2}\sqrt{\frac{3V}{\epsilon}}(3\epsilon - 2\eta). \qquad 24.$$

Thus, in slow-roll models, one expects $I_0 \lesssim 10^{-6}$ (unless for some unforeseen reason ϵ is extremely small and η is not), too small to be observed. A larger non-Gaussian signal may conceivably arise if there is a glitch in the inflaton potential, but even this non-Gaussianity would be extremely small (L Wang, M Kamionkowski, manuscript in preparation). Detection of nonzero I_0 would thus rule out the simplest slow-roll models.

Note that the theory predicts that the primordial distribution of perturbations is Gaussian. When the Universe becomes matter-dominated, and density perturbations undergo gravitational amplification, an initially Gaussian distribution will become non-Gaussian (149). Such departures from initial Gaussianity have a specific form and may be probed as consistency checks of inflation with galaxy surveys that probe the matter distribution today.

3.5 Brief Overview of Models

A huge literature is devoted to the construction of inflationary models (for a comprehensive review, see 60). Here we follow the classification of Dodelson et al (150). Models can be regarded as either large-field, small-field, or hybrid models. Linear models live at the border of large- and small-field models. In large-field (small-field) models, the inflaton moves a distance $\Delta\phi$ that is large (small) compared with the Planck mass during inflation. Hybrid models introduce a second scalar field and allow a broader range of phenomenology.

The models can be distinguished experimentally by the values of V, ϵ, and η that they predict, or equivalently by the set of V, r, and n_s, as shown in Figure 2.

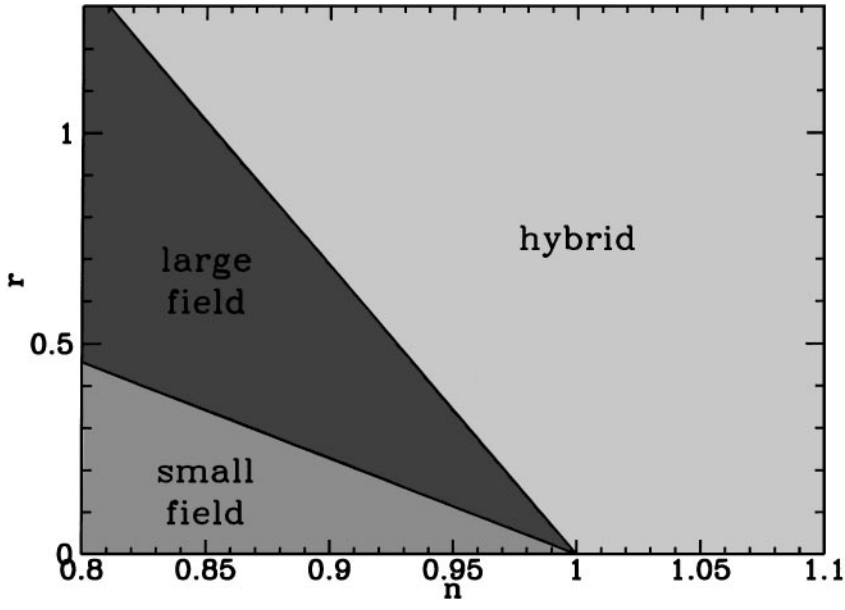

Figure 2 Regions in the n_s–r plane occupied by the various classes of inflationary models. (From References 150, 151; their n is our n_s.)

Examples of large-field models are single-field models with polynomial potentials, $V(\phi) \propto (\phi/\mu)^p$ (with $p > 1$), or in the $p \to \infty$ limit, exponential potentials, $V(\phi) \propto \exp(\phi/\mu)$.[4] The potentials in these models resemble qualitatively the potential shown in Figure 1*a*. These models have $V'' > 0$ and predict $\epsilon = [p/(p-2)]\eta > 0$ and $r \simeq 7[p/(p+2)](1-n_s)$. Thus, a large tensor amplitude is expected for large p (and therefore for exponential potentials as well) and for a sufficiently large deviation of n_s from unity.

Figure 1*b* shows a potential typical of a small-field model. These are the types of potentials that often occur in spontaneous symmetry breaking and can be approximated by $V(\phi) \propto [1-(\phi/\mu)^p]$. These models have $V'' < 0$. Demanding that the field move a distance that is small compared with $m_{\rm Pl}$ requires that $(\phi/\mu) \ll 1$, and in this limit, $\epsilon = [p/2(p-1)]|\eta|(\phi/\mu)^p \ll \eta$, $\eta < 0$, and $r \simeq 7(1-n_s)\epsilon/|\eta|$. Note that the slow-roll condition $\phi \ll \mu$ implies that $\epsilon \ll 1$, so $\epsilon \ll \eta$. It thus follows that $n_s \simeq 1+2\eta$, and that the tensor amplitude in these models is expected to be very small. Note that both small- and large-field models predict $n_s < 1$.

Linear models live at the border of small- and large-field models. They have potentials $V(\phi) \propto \phi$ (i.e. they have $V'' = 0$) and predict $\epsilon = -\eta > 0$ and $r \simeq (7/3)(1-n_s)$.

[4]Exponential potentials are sometimes referred to as power-law inflation, since the scale factor grows as a power law during inflation in these models.

Although hybrid models generally involve multiple scalar fields, they can be parameterized by a single-field model with a potential $V \propto [1 + (\phi/\mu)^p]$. These models have $\epsilon > 0$ and

$$\frac{\eta}{\epsilon} = \frac{2(p-1)}{p}\left(\frac{\phi}{\mu}\right)^{-p}\left[1 + \frac{p-2}{2(p-1)}\left(\frac{\phi}{\mu}\right)^{p}\right] > 0. \qquad 25.$$

Unlike small- or large-field models, hybrid models can (although are not required to) produce blue spectra, $n_s > 1$. Although both r and n_t depend only on ϵ and are thus related, there is no general relation between r and n_s in hybrid models. The tensor amplitude is only constrained to be smaller than it is in exponential models.

4. COSMIC MICROWAVE BACKGROUND TESTS OF INFLATION

Photons from overdense regions at the surface of last scatter are redder, since they must climb out of deeper potential wells [the Sachs-Wolfe effect (20)]. However, this is really only one of a number of physical mechanisms that give rise to temperature perturbations. We have also mentioned that if primordial perturbations are adiabatic, then the gas in deeper potential wells is hotter, and this partially offsets the reddening due to the depth of the potential. Density perturbations induce peculiar velocities, and these also produce temperature perturbations via Doppler shifts. Growth of the gravitational potential near the CMB surface of last scatter can produce temperature anisotropies (152) [the early-time integrated Sachs-Wolfe (ISW) effect], and so can the growth of the gravitational potential at late times in a flat cosmological-constant (153) or open (104) Universe (the late-time ISW effect).

Modern calculations of the CMB power spectra (the C_l) take into account all of these effects. The cosmological perturbation theory underlying these calculations has been reviewed (154–156), and solution of the Boltzmann equations for the observed angular distribution of CMB photons is discussed elsewhere (157–159). Such calculations for the CMB power spectra from density perturbations were developed in a series of pioneering papers from 1970 until the late 1980s (93, 113, 160–165), and these calculations have been refined extensively in the post-*COBE* era. Similar calculations can also be carried out for the CMB power spectra from gravitational waves (80, 82, 112, 166–172).

The calculations for both scalar and tensor power spectra require solution of a series of several thousand coupled differential equations for the perturbations to the spacetime metric, densities and velocities of baryons and cold dark matter (CDM), and the moments of the CMB photon and neutrino distributions. A code for carrying out these calculations (that required several hours for each model) was made publicly available (173). Hu & Sugiyama (174) came up with useful semianalytic fits to the numerical calculations that provided some physical intuition into the numerical results. More recently, Seljak & Zaldarriaga (81, 159) developed

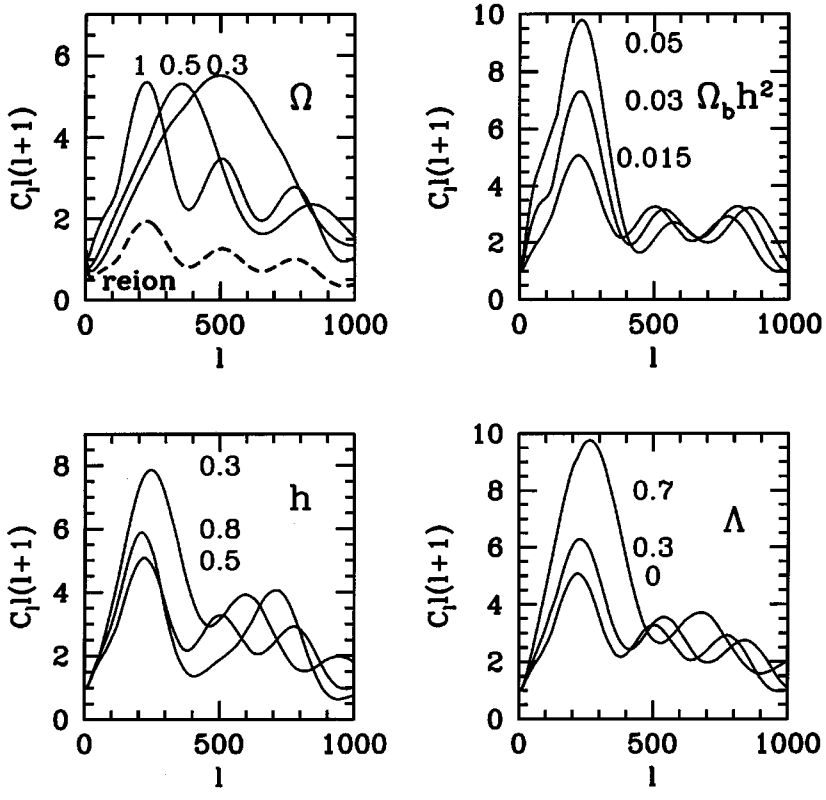

Figure 3 Theoretical predictions for cosmic-microwave-background temperature angular power spectra as a function of multipole moment l for models with primordial adiabatic perturbations. Each graph shows the effect of varying one of these parameters. In the *right lower panel*, $\Omega \equiv \Omega_0 + \Omega_\Lambda = 1$. (From Reference 175.)

a line-of-sight approach that speeded up the numerical calculations by several orders of magnitude. A code (CMBFAST) was made publicly available and has become widely used.

Given the values of the classical cosmological parameters (e.g. the nonrelativistic matter density Ω_0, cosmological constant Ω_Λ, and baryon density Ω_b, all in units of the critical density, and the Hubble parameter h in units of 100 km sec^{-1} Mpc^{-1}), and primordial scalar and tensor power spectra, $P_s(k)$ and $P_t(k)$, it is straightforward to calculate the C_l with the machinery described above. Figure 3 shows results of such calculations for models with a Peebles-Harrison-Zeldovich (i.e. $n_s = 1$) power spectrum of primordial adiabatic perturbations. Each panel shows the effect of independent variation of one of the cosmological parameters. As illustrated, the height, width, and spacing of the acoustic peaks in the angular spectrum depend on these (and other) cosmological parameters.

The wiggles[5] come from oscillations in the photon-baryon fluid at the surface of last scatter. Consider an individual Fourier mode of an initial adiabatic density perturbation. Because the density perturbation is nonzero initially, this mode begins at its maximum amplitude. The amplitude remains fixed initially when the wavelength of the mode is larger than the Hubble radius. When the Universe has expanded enough that the Hubble radius becomes larger than the wavelength of this particular mode, then causal physics can act, and the amplitude of this Fourier mode begins to oscillate as a standing acoustic wave (176). Because modes with smaller wavelengths come within the horizon earlier and oscillate more rapidly, they have at any given time undergone more oscillations than longer-wavelength modes have. The peaks evident in Figure 3 arise because modes of different wavelength are at different points of their oscillation cycles (177). The first peak corresponds to the mode that has had just enough time to come within the horizon and compress only once. The second peak corresponds to the mode that is at its maximum amplitude after the first compression, and so forth.

4.1 Determination of the Geometry

These acoustic peaks in the CMB temperature power spectrum can be used to determine the geometry of the Universe (178). The angle subtended by the horizon at the surface of last scatter is $\theta_H \sim \Omega^{1/2}\ 1^\circ$, where $\Omega = \Omega_0 + \Omega_\Lambda$ is the total density (objects appear to be larger in a closed Universe than they would be in a flat Universe and smaller in an open Universe than they would be in a flat Universe). Moreover, the peaks in the CMB spectrum are due to causal processes at the surface of last scatter. Therefore, the angles (or values of l) at which the peaks occur determine the geometry of the Universe. This is illustrated in the top left panel of Figure 3, where the CMB spectra for several values of Ω_0 are shown. As illustrated in the other panels, the angular position of the first peak is relatively insensitive to the values of other undetermined (or still imprecisely determined) cosmological parameters such as the baryon density, the Hubble constant, and the cosmological constant.

Small changes to the spectral index n_s tilt the entire spectrum slightly to smaller (larger) l for $n_s < 1$ ($n_s > 1$), and the location of the first peak is only weakly affected. Gravitational waves would only add to the temperature power spectrum at $l \ll 200$ (as discussed below in Section 4.4). Therefore, although gravitational waves could affect the height of the peaks relative to the normalization at small l, the locations would not be affected. It is plausible that an early generation of star formation released a sufficient flux of ionizing radiation to at least partially reionize the Universe, and if so, these ionized electrons would rescatter some fraction τ

[5]These are sometimes referred to inaccurately as Doppler peaks but are more accurately referred to as acoustic peaks. They are sometimes called Sakharov oscillations in honor of the scientist who first postulated the existence of photon-baryon oscillations in the primordial plasma (176). The existence of these peaks in the CMB power spectrum was, to the best of our knowledge, first identified by Sunyaev & Zeldovich (177) and Peebles & Yu (113).

of the CMB photons. A variety of theoretical arguments suggest that a fraction $\tau = \mathcal{O}(0.1)$ of CMB photons were rescattered (178–180) (and the amplitude of anisotropy at degree scales observed already supports this). Although reionization would damp the peaks by a factor $e^{-2\tau}$, as indicated by the curve labeled "reion" in the top left panel of Figure 3 (but note that the figure assumes $\tau = 1$), the location of the peaks would remain unchanged. Therefore, if peak structure is observed in the CMB power spectrum, determination of the location of the first peak will provide a robust determination of the geometry of the Universe (178).

4.1.1 Open Inflation

The most distinctive signature of an open-inflation model would be a low-Ω CMB power spectrum from adiabatic perturbations such as one of those shown in the top left panel of Figure 3, in which the first peak is shifted to larger l. Open inflation would also produce an increase in large-angle anisotropy from the integrated Sachs-Wolfe effect (103, 104), but different open-inflation models make different predictions about the large-angle anisotropy. Moreover, determination of the CMB power spectrum at these large angular scales is cosmic-variance limited, so it is unlikely that large-angle CMB anisotropies alone will be able to provide a robust test of open-inflation models. The ISW effect may alternatively be identified by cross-correlation of the CMB with some tracer of the mass density along the line of sight (181, 182), such as the X-ray background (12, 183) or possibly weak-lensing maps (184) (as discussed further in Section 6.3).

4.2 Adiabatic Versus Isocurvature Modes

The physics described above yields a distinctive pattern in the peak structure of the CMB power spectrum, and this leads to an important test of inflation. If primordial perturbations are isocurvature rather than adiabatic, then when a given Fourier mode comes within the horizon and begins to oscillate, it begins to oscillate from its minimum (rather than maximum) amplitude. Thus, the phase of its oscillation differs by $\pi/2$ from what it would be if the perturbation were adiabatic. As a result, the locations of the peaks in the CMB power spectrum in isocurvature models differ in phase from what they would be in adiabatic models (185–187), as shown in Figure 4. It has also been shown that the relative locations of the higher peaks differ in adiabatic and isocurvature models, independent of the shifts in the locations of the peaks owing to the geometry (188).

4.2.1 Axion Inflation

When the matter power spectrum is normalized to the amplitude of galaxy clustering, isocurvature models with nearly scale-invariant primordial power spectra (e.g. axion isocurvature or "axion inflation" models) produce roughly six times the CMB anisotropy seen by *COBE* (51, 52) (since there is no cancellation between the effects of the intrinsic temperature and the potential-well depth at the surface of last scatter) and are thus ruled out.

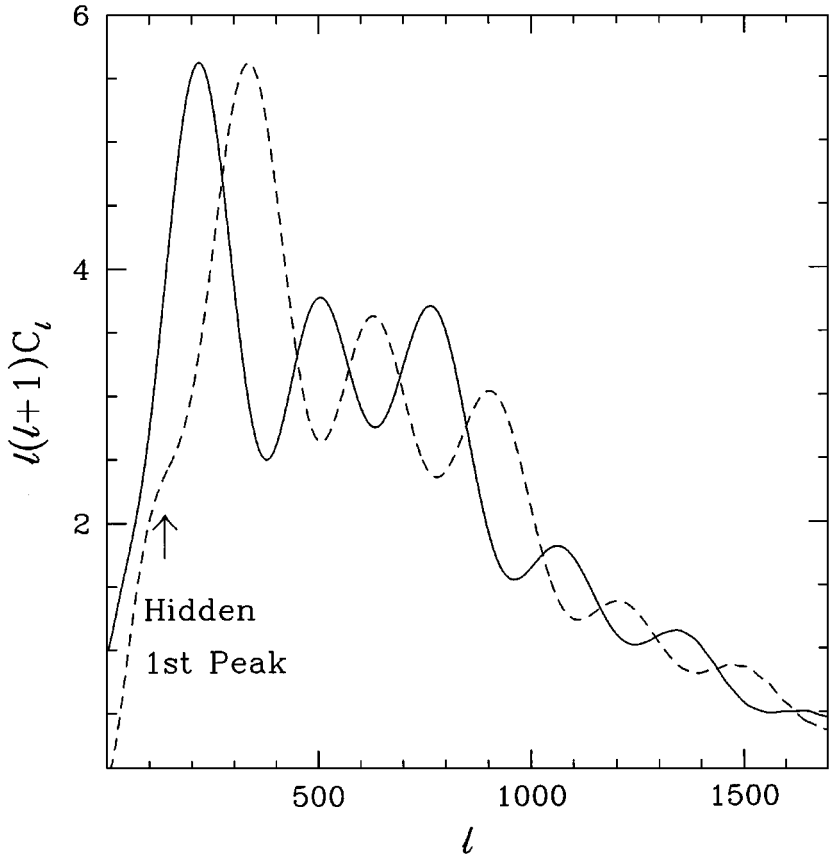

Figure 4 The angular power spectrum for an inflationary model with primordial adiabatic perturbations and for another with primordial isocurvature perturbations. *Solid line*, cold dark matter and inflation; *dashed line*, axion isocurvature. (From Reference 186.)

4.3 Coherent Perturbations and Polarization

Each Fourier component of the density field induces a Fourier component of the peculiar-velocity field, and the oscillations of these peculiar velocities are out of phase with the oscillations in the density perturbation (just as the velocity and position of a harmonic oscillator are out of phase). These peculiar velocities induce temperature anisotropies (via the Doppler effect) that are thus out of phase with those from density perturbations. This Doppler effect fills in the troughs in the $C_l^{\rm TT}$, which would otherwise fall to zero.

The CMB polarization is related to the peculiar velocity (189), so the peaks in the polarization power spectrum (from density perturbations) are out of phase from those in the temperature power spectrum and fall close to zero (Figure 5).

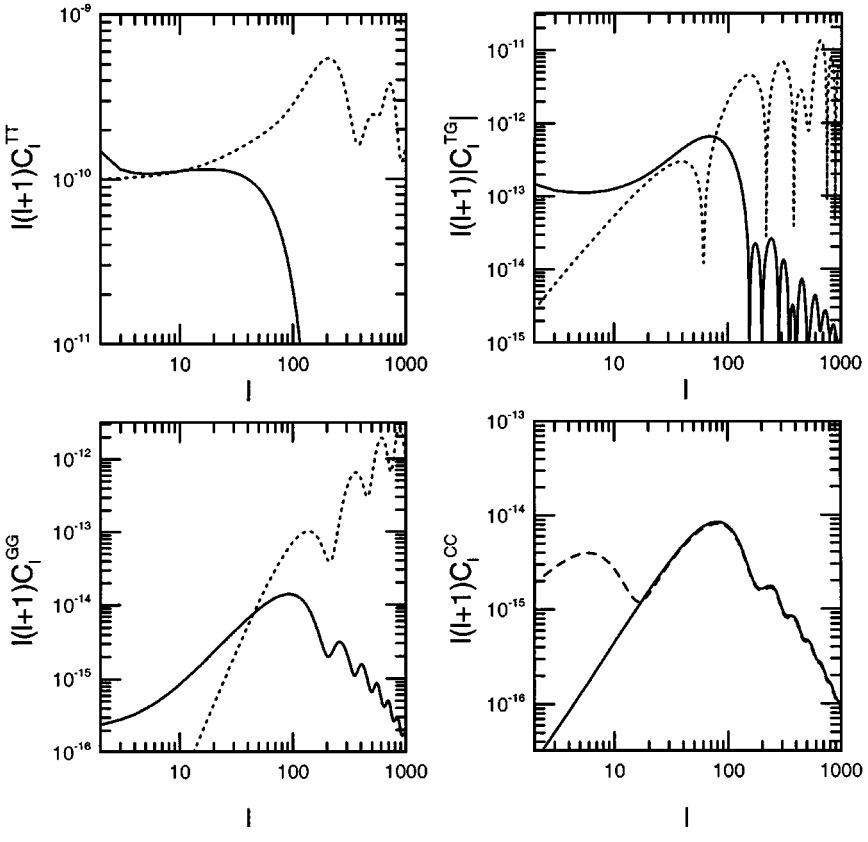

Figure 5 Theoretical predictions for the four nonzero cosmic-microwave-background temperature-polarization spectra as a function of multipole moment l. *Solid curves* are the predictions for a *COBE*-normalized inflationary model with no reionization and no gravitational waves for $h = 0.65$, $\Omega_b h^2 = 0.024$, and $\Lambda = 0$. *Dotted curves* are the predictions that would be obtained if the *COBE* anisotropy were due entirely to a stochastic gravity-wave background with a flat scale-invariant spectrum (with the same cosmological parameters). The panel for $C_l^{\rm CC}$ contains no dotted curve because scalar perturbations produce no "C" polarization component; instead, the *dashed line* in the *bottom right panel* shows a reionized model with optical depth $\tau = 0.1$ to the surface of last scatter. (From Reference 191.)

This relative positioning of the temperature and polarization peaks is a signature of coherent perturbations (rather than those produced, for example, by the action of topological defects, as discussed below) (187). Zaldarriaga & Spergel (190) argue that the location of the first peak in the polarization power spectrum provides a test of primordial perturbations as the origin of structure and thus of inflation. If some causal mechanism (such as topological defects) produced large-scale structure, the the first peak would have to occur at smaller angular scales in order to be within

the horizon at the surface of last scatter (see below). A peak so close to the causal horizon could only occur with super-horizon-sized primordial perturbations, for which inflation is the only causal mechanism.

4.4 Polarization and Gravitational Waves

Gravitational waves are usually detected by observation of the motion they induce in test masses. The photon-baryon fluid at the surface of last scatter acts as a set of test masses for detection of gravitational waves with wavelengths comparable to the horizon, such as those predicted by inflation. These motions are imprinted onto the temperature and polarization of the CMB. Figure 5 (*top left panel; solid curve*) shows the temperature power spectrum for a *COBE*-normalized flat scale-invariant ($n_t = 0$) spectrum of gravitational waves. It is flat and relatively featureless for $l \lesssim 70$. The dropoff at $l \gtrsim 70$ occurs because the amplitudes of gravitational-wave modes that enter the horizon before the epoch of last scatter have decayed with the expansion of the Universe. Unfortunately, cosmic variance from scalar perturbations provides a fundamental limit to the sensitivity of CMB temperature maps to tensor perturbations (99). Even if all other cosmological parameters are somehow fixed, a perfect temperature map can never detect an inflaton-potential height smaller than one tenth the upper limit provided by *COBE* (175). More realistically, the effects of gravitational waves and reionization on the temperature power spectrum are similar and difficult to disentangle, so improvements to the current *COBE* sensitivity to gravitational waves is unlikely with a temperature map alone.

However, with a polarization map of the CMB, the scalar and tensor contributions to CMB polarization can be geometrically decomposed in a model-independent fashion, and the cosmic-variance limit present in temperature maps can thereby be circumvented (79, 81, 83). Scalar perturbations have no handedness, so they cannot give rise to a curl component. On the other hand, tensor perturbations do have a handedness, so they induce a curl component. Therefore, if any curl coefficient, $a^C_{(lm)}$, is found to be nonzero, it suggests the presence of gravitational waves.[6]

To illustrate, Figure 5 shows the four nonzero temperature-polarization power spectra. The solid curves correspond to a *COBE*-normalized inflationary model with no gravitational waves. The dotted curves show the spectra for a *COBE*-normalized stochastic gravitational-wave background.

4.4.1 Detectability of Gravitational Waves: Curl Component Only

Consider a mapping experiment that measures the polarization on the entire sky with a temperature sensitivity s (which has units $\mu\text{K}\sqrt{\text{sec}}$) for a time t_{yr} years. If only the curl component of the polarization is used to detect tensor perturbations,

[6]A curl component may also arise from vector perturbations. Although topological-defect models may excite such modes, they do not arise in inflationary models.

then such an experiment can distinguish a tensor signal from a null result at the 2σ level if the inflaton potential height is (191)

$$V \gtrsim (4 \times 10^{15}\,\mathrm{GeV})^4\, t_{\mathrm{yr}}^{-1}\, (s/\mu\mathrm{K}\,\sqrt{\mathrm{sec}})^2. \qquad 26.$$

Equation 26 indicates that to access an inflaton-potential height not already excluded by *COBE* requires a detector sensitivity $s \lesssim 35\, t_{\mathrm{yr}}^{1/2}\,\mu\mathrm{K}\sqrt{\mathrm{sec}}$. To compare this with realistic values, the effective sensitivity of MAP is $s \simeq 150\, t_{\mathrm{yr}}^{1/2}\,\mu\mathrm{K}\sqrt{\mathrm{sec}}$ and that for Planck is about $s \simeq 35\, t_{\mathrm{yr}}^{1/2}\,\mu\mathrm{K}\sqrt{\mathrm{sec}}$, and technological developments have improved the detector sensitivity roughly an order of magnitude per decade for the past several decades. Even better sensitivities may be possible with deep integration on a smaller region of the sky.

4.4.2 Reionization

In some sense, Equation 26 is conservative because even a small amount of reionization will significantly increase the polarization signal at low l [indicated by the *dashed curve* in the CC panel of Figure 5 (192)]. If $\tau = 0.1$, then the sensitivity to tensor modes is increased by roughly a factor of five (191).

4.4.3 Full Polarization and Temperature Spectra

Although searching only for the curl component provides a model-independent probe of tensor modes, a stochastic gravitational-wave background leads to specific predictions for all four nonzero temperature-polarization power spectra (Figure 5). Fitting an inflationary model to the entire set of temperature and polarization power spectra can improve tensor detectability, especially at poorer sensitivities, albeit with the introduction of some model dependence. For detector sensitivities $s \gtrsim 15\, t_{\mathrm{yr}}^{1/2}\,\mu\mathrm{K}\sqrt{\mathrm{sec}}$, the sensitivity to a tensor signal is improved by factors of a few or so (191), depending on the cosmological model, whereas for detector sensitivities $s \lesssim 15\, t_{\mathrm{yr}}^{1/2}\,\mu\mathrm{K}\sqrt{\mathrm{sec}}$, the sensitivity is attributable almost entirely to the CC power spectrum and approaches the limit in Equation 26.

4.4.4 Measurement of Inflationary Observables

Several authors have addressed the question of how precisely the inflationary observables can be reconstructed in the case of a positive detection of the stochastic gravitational-wave background with only a temperature map (150, 175, 193, 194) and with a polarization map as well (151, 195, 196). We follow the discussion of Reference (151).

Figure 6 shows the 2σ error ellipses that would be obtained by the Planck Surveyor using the temperature only (i.e. the cosmic-variance limit) and with the polarization, assuming a gravitational-wave background with $r \simeq 0.01$ and $n_s \simeq 0.9$. (A larger gravitational-wave amplitude would be detectable, as shown in Figures 3–6 in Reference 151.) The 2σ cosmic-variance limit from a temperature map is shown, as is the 2σ constraint to the parameter space expected for Planck (with polarization). Although such a tensor amplitude cannot be distinguished from a

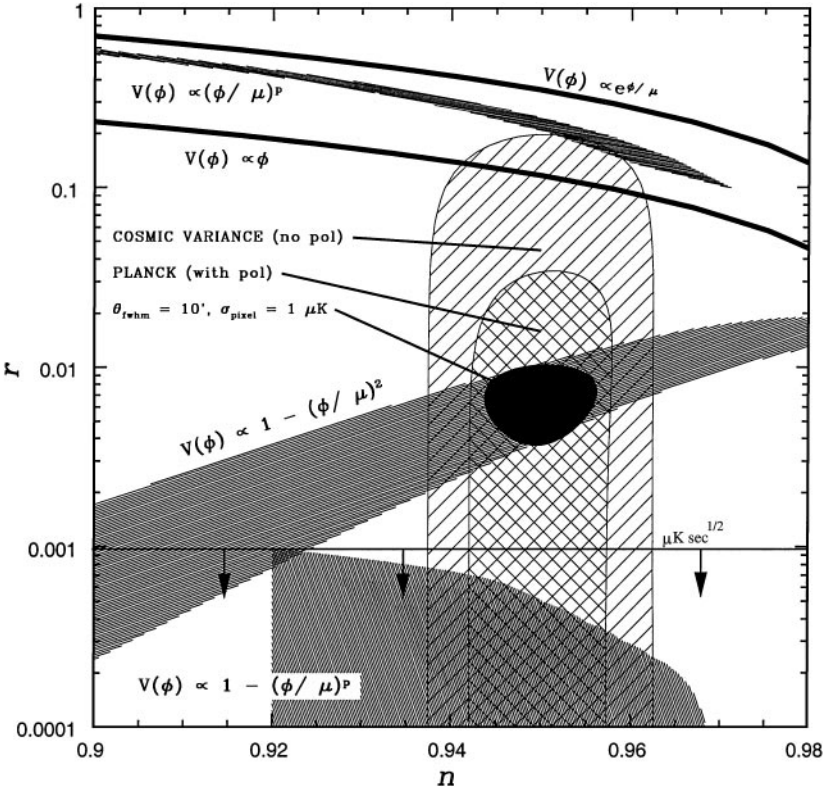

Figure 6 Simulated 2σ error ellipses that would be obtained by a cosmic-variance-limited temperature map, the Planck Surveyor (with polarization), and an experiment with three times the sensitivity of Planck. This assumes an inflationary model with $r = 0.01$ and $n_s = 0.95$ and an optical depth to the surface of last scatter of $\tau = 0.05$. Shaded regions indicate the predictions of various inflationary models. Solid horizontal curve indicates the regions of this logarithmic parameter space that would be accessible with a hypothetical polarization experiment with 30 times the Planck instrumental sensitivity (191). Even better sensitivities may be possible with deep integration on a smaller region of the sky. (From Reference 151.)

null result, the figure shows (*dark shaded region*) that a hypothetical experiment with three times the Planck polarization sensitivity could discriminate between such a tensor signal and a null result. It would also discriminate between a single small-field model and a hybrid model. Of course, the sensitivity to tensor modes can be improved as the instrumental sensitivity is improved, as indicated by Equation 26. For example, the thin horizontal line at $r = 0.001$ shows the smallest value of r that could be distinguished from a null result by a hypothetical one-year experiment with an instrumental sensitivity $s = \mu\text{K}\sqrt{\text{sec}}$, roughly 30 times that of

Planck (191). A null result from such an experiment would suggest that if inflation occurred, it would have required a small-field model.

4.5 Gaussianity

The prediction of primordial Gaussianity or of some specific small deviations from Gaussianity can be probed with the CMB angular bispectrum or higher n-point correlation functions discussed above. A nonzero large-angle CMB bispectrum may arise from the integrated Sachs-Wolfe effect if there is a cosmological constant (146). Such a bispectrum, as well as that probed by the Sunyaev-Zeldovich effect, may be discernible via cross-correlation between gravitational-lensing maps and the CMB (197). A more powerful test of inflation models may arise from probing the bispectrum induced by nonlinear evolution at the surface of last scattering (S Winitzki, A Kosowsky, DN Spergel, manuscript in preparation).

Ferreira et al and Pando et al (97, 148) recently claim to have already found some signature of non-Gaussianity in the *COBE* maps. In particular, Ferreira et al (148) find $I_l^3 \sim 1$ for $l \sim 16$ [although it is still not clear if the effect is real (198)]. If this result is correct, then the simplest slow-roll inflation models are not viable (see Equation 24).

5. TOPOLOGICAL-DEFECT MODELS

The leading alternative to structure-formation models based on inflation have been those based on topological defects, particularly cosmic strings (33–36, 199), global monopoles (40, 41), domain walls (27, 37), and textures (38, 39) (for reviews, see 200, 201). Defect models postulate a phase transition in the early Universe that leads to a vacuum manifold with nontrivial topology; the type of defect depends on the specific topology (see 199 for a review). Since defect formation is a process governed by causal physics, the vacuum state of the field must be uncorrelated on scales larger than the horizon at the time of the phase transition, guaranteeing the formation of defects with a characteristic length scale of the horizon [the "Kibble mechanism" (32)].

The simplest defects are domain walls, which arise in theories with a discrete symmetry. Domain-wall models are not viable because their energy densities are large enough to produce larger CMB temperature fluctuations than those observed (31, 202, 203).

Cosmic strings are stable defects that arise in gauge models with a $U(1)$ symmetry. They produce density perturbations by their gravitational interactions with ordinary matter. Global-monopole and texture models are unstable defects that arise in models with a perfect global symmetry. They provide two mechanisms for structure formation: (*a*) the energy-density provided by misalignment of scalar fields as causally disconnected regions of the Universe come into causal contact, and (*b*) the explosive events that occur when the topological defects unwind.

Nontopological texture models (29, 30, 204, 205) postulate an even higher global symmetry and seed structure via scalar-field alignment even though no topological defects are formed. Generically, one expects quantum gravity to violate global symmetries to the level that would render global-monopole, texture, and scalar-field-alignment models unworkable (206, 207). If it can be shown that such models do seed large-scale structure, valuable information on Planck-scale physics will thus be provided.

5.1 Cosmic-Microwave-Background Power Spectra in Defect Models

In contrast to inflationary models, which lay down an initial spectrum of density perturbations, defect models produce perturbations actively throughout the history of the Universe. This generally leads to loss of coherence in the perturbations and a corresponding smoothing of the acoustic peaks (208–210). Defect-model perturbations are also causal, being generated by physical processes inside the horizon (211–215). And finally, primordial perturbations in defect models more closely resemble those in primordial-isocurvature models than in adiabatic models (211, 214, 216). Moreover, the action of topological defects generically produces vector and tensor perturbations, which increase the anisotropy on small angular scales (54, 56), further suppressing any peak structure [although it may produce some characteristic C polarization (217)].

Until recently, different groups obtained different results about the extent to which acoustic peaks exist in defect models, and under what circumstances (212, 213, 218–220). Calculations of CMB power spectra based on large simulations of a variety of defect sources have now been performed (54, 56, 221) (see Figure 7 for some). The numerical results indicate that the acoustic peaks are indeed washed out.

At this point, it appears that the simplest defect models are inconsistent with the observed CMB fluctuations and the large-scale structure traced by galaxy surveys. Although this could have been inferred from the generic arguments discussed in the Introduction (53), it has been supported by these more recent precise calculations (54–56). The question now is whether any more complicated (or "sophisticated") defect models are viable. Albrecht et al (222, 223) have suggested that a cosmological constant might help improve concordance with current data. However, suppose the CMB temperature spectrum continues to look increasingly like that caused by inflation (i.e. with identifiable acoustic peaks). If so, can any defect model reproduce such a power spectrum? Turok (213) produced a power spectrum with a phenomenological defect model that closely mimicked an inflation power spectrum, and Hu (224) has invented a similar isocurvature model. But it is hard to see how to position the acoustic peaks in isocurvature-like models at the same angular scales as in adiabatic models without some very artificial initial conditions (214, 225, 226). It is also difficult to simultaneously account for the fluctuation amplitude in the CMB and galaxy surveys, unless there is a breaking of scale invariance [possibly from some finite breaking of the global symmetry (206, 207)].

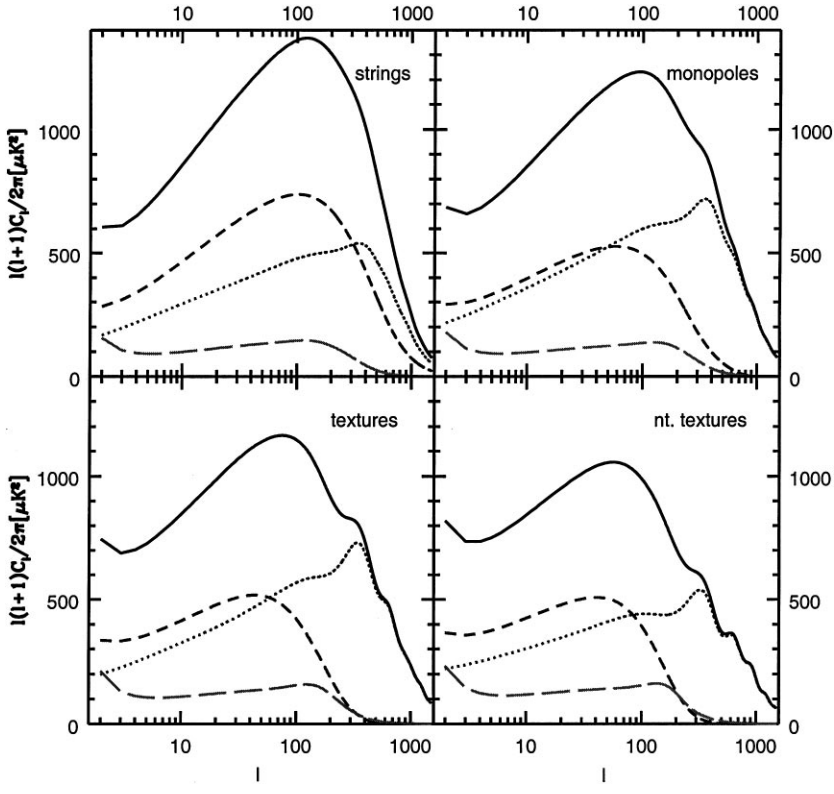

Figure 7 Cosmic-microwave-background power spectra from topological-defect models. Solid line, total; dotted, scalar; short-dashed, vector; long-dashed, tensor. (From Reference 217.)

It may, in fact, be possible to construct some causal models that produce peaks in the CMB power spectrum (215, 216), but it is unclear whether fluctuations that mimic a specific inflationary model can be produced, particularly when additional constraints from polarization are taken into account. Finally, it should be noted that hybrid models with both primordial adiabatic perturbations and defects have been entertained (227–229).

5.2 Non-Gaussianity

Topological-defect models may also be distinguished by the non-Gaussian signatures they produce in the CMB. Because the evolution of topological defects is nonlinear, they generically produce non-Gaussian structures in the CMB. Put another way, the production of defects via the Kibble mechanism is a Poisson process; the number of defects within any volume in the Universe is Poisson distributed. The central-limit theorem guarantees that as the number density of defects becomes large, the distribution should become increasingly Gaussian. Thus cosmic-string

models should look more like Gaussian perturbations than textures should, since the Kibble mechanism produces roughly one texture per 25 Hubble volumes as opposed to roughly one cosmic string per Hubble volume (230–234). In the large-N limit of the $O(N)$ sigma model, the clearest signature of non-Gaussianity from scalar-field alignment is at large angular scales (205); on small distance scales, the theory looks roughly Gaussian. Constraints to non-Gaussianity from the galaxy distribution have already posed problems for scalar-field alignment models for several years. Moreover, since defects are coherent structures, they can produce corresponding coherent structures in the CMB temperature anisotropy. For example, a cosmic string can produce a linear discontinuity in the CMB temperature (235), which can be searched for most efficiently through statistics tailored to match this particular signal (236–238). Textures might form large hot spots (239, 240).

6. DARK MATTER

The CMB can potentially provide a wealth of information about the dark matter known to dominate the mass of the Universe. The smallness of the amplitude of CMB temperature fluctuations has for a long time provided some of the strongest evidence for the existence of dark matter. In a low-density Universe, density perturbations grow when the Universe becomes matter-dominated and end when it becomes curvature-dominated. If the luminous matter ($\Omega_{\rm lum} \sim 10^{-3}$) were all the mass in the Universe, then the epoch of structure formation would be too short to allow density perturbations to grow from their early-Universe amplitude, fixed by *COBE*, to the amplitude observed today in galaxy surveys.

More precise measurements of the CMB power spectrum hold the promise of providing much more detailed information about the properties and distribution of dark matter. There are currently several very plausible dark-matter candidates that arise from new particle physics, and some evidence has already been claimed for the existence of several of these. For example, some observational evidence points to the existence of a cosmological constant (241–243), and the LSND experiment suggests that massive neutrinos may constitute a significant fraction of the mass of the Universe (244, 245). Moreover, there are good arguments that a significant fraction of the mass in galactic halos is made of some type of cold-dark-matter particle, e.g. weakly interacting massive particles (WIMPS) (246) or axions (247, 248).

6.1 Cold Dark Matter

A number of dynamical measurements suggest that the nonrelativistic-matter density is $\Omega_0 \gtrsim 0.1$, whereas big-bang nucleosynthesis suggests a baryon density of $\Omega_b \lesssim 0.1$. Observations of X-ray emission from galaxy clusters suggest that the nonrelativistic matter in clusters outweighs the baryonic matter by a factor of three or more (249), and weak lensing of background galaxies by clusters directly reveals large amounts of dark matter (250). This evidence strongly indicates the

existence of some nonbaryonic dark matter. By fitting the power spectra from MAP and Planck to theoretical predictions, one should simultaneously be able to determine both $\Omega_0 h^2$ and $\Omega_b h^2$ to far better precision than that obtained by current observations (175, 194, 195). If a substantial fraction of the mass in the Universe is in fact made of nonbaryonic dark matter [e.g. WIMPS (246) or axions (247, 248)], then it will become evident after MAP and Planck. Unfortunately, there is no way to discriminate between WIMPs and axions with the CMB.

6.2 Neutrinos

One of the primary goals of experimental particle physics is pursuit of a nonzero neutrino mass. Some recent (still controversial) experimental results suggest that one of the neutrinos may have a mass of $\mathcal{O}(5\,\mathrm{eV})$ (244, 245). There have been some arguments (again, still controversial) that such a neutrino mass is exactly what is required to explain apparent discrepancies between large-scale-structure observations and the simplest inflation-inspired standard-CDM model (251–256).

If the neutrino does indeed have a mass of $\mathcal{O}(5\,\mathrm{eV})$, then roughly 30% of the mass in the Universe is in the form of light neutrinos. These neutrinos will affect the growth of gravitational-potential wells near the epoch of last scatter, thus leaving an imprint on the CMB angular power spectrum (157, 257, 258). The effect of a light neutrino on the power spectrum is small, so other cosmological parameters that might affect the shape of the power spectrum at larger l must be known well. Eisenstein et al (259) argue that by combining measurements of the CMB power spectrum with those of the mass power spectrum measured by, for instance, the Sloan Digital Sky Survey, a neutrino mass of $\mathcal{O}(5\,\mathrm{eV})$ can be identified. The CMB may constrain the number of noninteracting relativistic degrees of freedom in the early Universe (175). Although weaker than the bound from big-bang nucleosynthesis (260, 261), the CMB probes a different epoch ($T \sim$ eV rather than $T \sim$ MeV) and may thus be viewed as complementary.

6.3 Cosmological Constant

Some recent evidence seems to point to the existence of an accelerating expansion, possibly due to a nonzero cosmological constant (241–243; for a review of the cosmological constant, see 262). The CMB may help probe the existence of a cosmological constant in a number of ways. As discussed above, if adiabatic perturbations are responsible for large-scale structure, then the position of the first acoustic peak in the CMB power spectrum provides a model-independent probe of the total density, $\Omega = \Omega_0 + \Omega_\Lambda$ (178). In contrast, supernova measurements of the Hubble diagram at large redshifts determine primarily the deceleration parameter $q_0 = \Omega_0/2 - \Omega_\Lambda$, so the two measurements together can give tight limits on both Ω_0 and Ω_Λ individually (263–268).

As the bottom panels of Figure 3 show, variations to Ω_0 and h affect the height and width of the first acoustic peak; the dependence is more precisely on the quantity $\Omega_0 h^2$. Thus, if the Hubble constant is known, then the CMB can determine Ω_0 and Ω (from the peak location) and therefore the cosmological constant Ω_Λ.

A cosmological constant may also be distinguished from the CMB via the additional large-angle anisotropy it produces via the ISW effect (153) from density perturbations at redshifts $z \lesssim$ few. If there is a cosmological constant, there should be a cross-correlation between the CMB temperature and some tracer of the mass distribution, e.g. the extragalactic X-ray background (12) or weak lensing (184), at these redshifts (181) [the same also occurs in an open Universe (182, 183)]. An experimental upper limit to the amplitude of this cross-correlation (12) can already be used to constrain Ω_0, with some assumptions about the bias of sources that give rise to the extragalactic X-ray background. If $\Omega_0 \simeq 0.3$ (either in an open or a flat cosmological-constant model), then these X-ray sources can be no more than weakly biased tracers of the mass distribution (183).

6.4 Rolling Scalar Fields

The supernova evidence for an accelerating expansion has engendered a burst of theoretical activity on exotic forms of matter with an equation of state $p < -\rho/3$ (i.e. the equation of state needed for $q_0 < 0$). The simplest possibility is of course a cosmological constant. However, as explained in Section 3.1, a rolling scalar field may also provide such an equation of state, provided the scalar field is not rolling too quickly. An almost endless variety of equations of state—and expansion histories—are possible in principle, given the freedom to choose the scalar-field potential and the initial conditions. This idea is variously referred to in the literature as rolling-scalar-field, variable-cosmological-constant, x-matter, generalized-dark-matter, loitering-Universe, and/or quintessence models (28, 269–277). Additional work has explored attractor solutions based on exponential potentials (278–283) or "tracker-field" solutions (284, 285) that attempt to explain why the matter density would be comparable to a scalar-field energy density today.

Because the expansion rate at decoupling in such models is the same as in cosmological-constant models with the same Ω_0, the peak structure in the CMB is virtually indistinguishable from that in cosmological-constant models (286). However, perturbations in the scalar field track perturbations to the matter density on large scales in such a way that the large-angle ISW effect that appears in cosmological-constant models is cancelled by the effect of scalar-field perturbations (276). Data from cosmological observations, particularly supernova measurements of the expansion history and measurements of the power spectrum through large galaxy surveys, may in principle be used to break these degeneracies (287, 288).

7. OTHER CONSTRAINTS ON PARTICLE PHYSICS

7.1 Decaying Particles

As discussed in Section 2.1, FIRAS limits to μ and y distortions limit the injection of energy into the early Universe and can thus be used to constrain the mass-lifetime

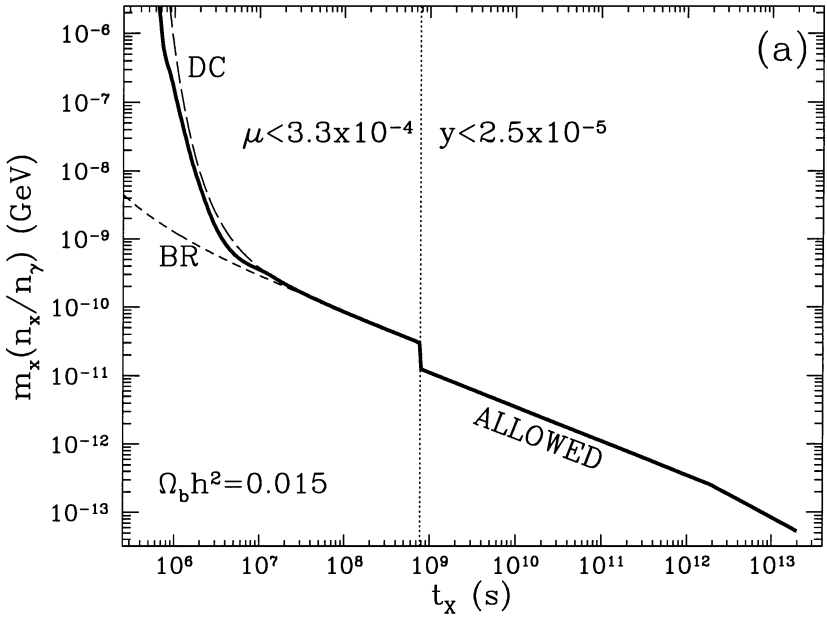

Figure 8 Constraints to the mass-lifetime plane for particles decaying to photons from FIRAS constraints to distortions to the CMB blackbody spectrum. The quantity n_X/n_γ is the initial ratio of the particle number density to the photon number density. Solid curve is the numerical result; dashed curves show various approximations. (From Reference 289.)

plane of particles that decay to electromagnetically interacting particles (as shown in Figure 8) (289, 290). The CMB power spectrum can also constrain decaying particles. For example, a neutrino of mass $\gtrsim$10 eV that decays to relativistic particles with a lifetime $\tau \simeq 10^{13-17}$ alters the expansion rate of the Universe between recombination and today and thus produces large-angle anisotropy (via the ISW effect) in disagreement with observations (291–293).

7.2 Time Variation of Fundamental Constants

A number of ideas for new physics postulate that some of the fundamental constants of nature, such as the fine-structure constant α, may actually be varying (for a review, see 294). Such a variation could be caused by the cosmological evolution of compact spatial dimensions in string theory or Kaluza-Klein theories (295–297) or through scalar fields coupled to electromagnetism (298). Limits of $|\Delta\alpha/\alpha| \lesssim 10^{-7}$ were provided by the natural nuclear reactor at Oklo (299, 300), and observations of atomic- and molecular-line positions at high redshifts (301) provide limits of $|\Delta\alpha/\alpha| < 3\times10^{-6}$ at redshifts less than 1 (302) and $|\Delta\alpha/\alpha| \lesssim 3\times10^{-4}$ at redshifts of 3 (303, 304). In fact, a detection of $\Delta\alpha/\alpha = -1.9 \pm 0.5 \times 10^{-5}$ has been

claimed on the basis of absorption lines at redshifts greater than 1 (305), but there are some potential problems with this result (304). Primordial nucleosynthesis can also provide a less useful model-dependent limit (306).

A change in α would affect the recombination rate of hydrogen and thus alter the redshift of last scatter. This effect on the CMB can potentially lead to upper limits on $|\Delta\alpha/\alpha|$ between 0.01 and 0.001 (307, 308) out to redshifts $z \simeq 1100$, much larger than those probed by quasar absorption spectra.

7.3 Topology of the Universe

The fundamental cosmological assumptions of homogeneity and isotropy require the Universe to be either the open, closed, or flat Friedmann-Robertson-Walker (FRW) model. However, if the assumption of anisotropy is incorrect, then the Universe may have some nontrivial topology (see 309 for a review). The open and flat FRW models have infinite volume, but a Universe with either zero or negative curvature can have finite volume if the Universe has nontrivial topology. A number of (somewhat imprecise) theoretical arguments suggest that a finite Universe is easier to explain than an open Universe (310) or could be used to explain the homogeneity of the Universe (311, 312).

If the volume of such a Universe is comparable to or less than that observable today, then there may be signatures in the CMB. Consider the simplest nontrivial topology (for a flat Universe), that of a toroid. If the Universe is a three-dimensional toroid, then two different directions on the sky will point to the same point in space, and there should be observable correlations between the CMB temperature at distant locations in the sky. Such models have essentially been ruled out by *COBE* (313–322).

Interest in negative-curvature models with nontrivial topology has reawakened recently because evidence seems to suggest $\Omega_0 \simeq 0.3 < 1$, and thus possibly an open Universe. If the Universe is negatively curved (hyperbolic), the spacetime volume element increases rapidly with distance, so that even if the volume of the Universe is close to the horizon volume, many copies of the Universe may still fit inside the horizon volume. Thus, none of the flat-Universe limits on topology apply to hyperbolic Universes (323). Furthermore, if the total density of the Universe is $\Omega \simeq 0.3$, the curvature scale is small enough so that a huge number of topologies exist that have proper volumes significantly smaller than the proper Hubble volume (324).

Because the surface of last scatter is spherical, matched pairs of temperature circles would appear in a negatively curved Universe with nontrivial topology (109, 324, 325) if the topology radius were smaller than the current horizon. Levin et al (326) propose searching for specific correlations between a given pixel and all others in a map. A null search for such correlations in the *COBE* maps ruled out a particular horn topology (327). Souradeep et al (328) claim that the *COBE* maps already rule out most hyperbolic Universes through this technique, although details have not been presented.

7.4 Primordial Magnetic Fields

Magnetic fields of strength 10^{-6} G are ubiquitous in our galaxy and in distant clusters of galaxies. All mechanisms for the origin of these magnetic fields postulate that they grew via some mechanism (e.g. dynamo or adiabatic compression) from small, primordial magnetic fields. However, the origin of these primordial seed fields remains a mystery. Many of the most intriguing hypotheses about the origin of these fields come from new ideas in particle theory. Proposed generation mechanisms include inflation (329–335), the electroweak (336, 337) or QCD phase transitions (338, 339), a ferromagnetic Yang-Mills vacuum state (340), charge asymmetry (341), and dilaton evolution (342).

Magnetic fields have several potentially measurable effects: Faraday rotation (343; A Mack, A Kosowsky, manuscript in preparation) and associated depolarization (344) of the original CMB polarization; magnetosonic waves that modify the acoustic oscillation frequencies (345); and Alfvén waves, which can amplify vector perturbations and induce additional correlations (346), and for which diffusion damping is decreased, thereby increasing CMB power at small scales (347). The Faraday rotation signals can be detected through the CC, TC, and GC power spectra they induce (348) (although these power spectra are frequency dependent). A recent analysis of the *COBE* maps has placed a limit on a homogeneous primordial field strength corresponding to $B_0 < 3.4 \times 10^{-9}(\Omega_0 h_{50}^2)^{1/2}$ G (349) by searching for the temperature pattern of a Bianchi type VII anisotropic spacetime (350, 351).

7.5 Large-Scale Parity Violation

It is usually assumed that gravity is parity-invariant. However, weak interactions are parity-violating (352, 353), and we surmise that the electroweak interactions are united with gravity at the Planck scale by some fundamental unified theory. Are there any remnants of parity-violating new physics in the early Universe? As discussed in Section 2.2.2, if either of the temperature-polarization cross-correlation moments $C_l^{\rm TC}$ or $C_l^{\rm TG}$ is nonzero, it signals cosmological parity breaking. Lue et al and Lepora (354, 355) discuss how a parity-violating term, $\phi F_{\mu\nu}\tilde{F}^{\mu\nu}$ (298, 330, 356), that couples a scalar field ϕ to the pseudoscalar $\vec{E}\cdot\vec{B}$ of electromagnetism could yield nonzero $C_l^{\rm TC}$ and $C_l^{\rm GC}$. Lue et al (354) also discuss a parity-violating term in the Lagrangian for gravitation that would yield an asymmetry between the density of right- and left-handed gravitational waves produced during inflation; such an asymmetry would also give rise to nonzero $C_l^{\rm TC}$ and $C_l^{\rm GC}$. These parity-breaking effects would produce frequency-independent $C_l^{\rm TC}$ and $C_l^{\rm GC}$, unlike the frequency-dependent effect of Faraday rotation.

7.6 Baryon Asymmetry

There are good theoretical and observational reasons to believe that our entire observable Universe is made of baryons and no antibaryons. But suppose

momentarily that the observable Universe consisted of some domains with antibaryons rather than baryons (see e.g. 357). If so, then particle-antiparticle annihilations at the interfaces of the matter and antimatter regions would release a significant amount of energy in γ-rays, thus heating the region and causing a y-distortion of the CMB spectrum of order $y \simeq 10^{-6}$ (358, 359). These distortions would appear in thin strips in the sky that could potentially be identified. However, the point is moot because limits on the diffuse extragalactic γ-ray background limit the size of our matter domain to be essentially as large as the horizon (359).

7.7 Alternative Gravity Models

We now know through a variety of experiments that general relativity provides an accurate accounting of observed gravitational phenomena. On the other hand, string theories generically predict at least some small deviation from general relativity, often in the form of scalar-tensor theories of gravity (360–364). The simplest of these is Jordan-Fierz-Brans-Dicke (more commonly, Brans-Dicke) theory (365–370). An inflation theory ("extended inflation") based on Brans-Dicke gravity (371, 372) was ruled out by the isotropy of the CMB (373, 374), although models based on more complicated scalar-tensor theories ("hyperextended inflation") have also been considered (375–378).

Brans-Dicke theory includes a scalar field Φ and a new parameter ω. As $\omega \to \infty$, the theory recovers general relativity (in some sense). Solar-system constraints from Viking spacecraft data limit $\omega \geq 500$ (for a review, see 379) and recent Very Long Baseline Interferometry (VLBI) measurements of time delays of millisecond pulsars may further raise this limit (380). In cosmological models based on Brans-Dicke theories, general relativity is an attractor solution (381, 382), so gravity could have conceivably differed from general relativity in the early Universe even if it resembles general relativity today.

Because the expansion rate and growth of gravitational-potential perturbations are different in alternative-gravity theories, the precise predictions for CMB power spectra should be different in these models. The epoch of matter-radiation equality is altered in Brans-Dicke theories, and this may produce an observable signal in forthcoming precise CMB maps (383). Cosmological perturbation theory in scalar-tensor theories has been worked out (113, 384–386) and the CMB power spectra calculated (X Chen, M Kamionkowski, manuscript in preparation). If the scalar-field time derivative $\dot{\Phi}$ is fixed to be small enough to be consistent with big-bang-nucleosynthesis constraints (387–390) and $\omega > 500$, then the differences between the general-relativistic and Brans-Dicke predictions are small, although conceivably detectable with the Planck Surveyor. Of course, the scalar-field evolution may be significantly different in more sophisticated scalar-tensor theories, but predictions for these models have yet to be carried out.

7.8 Cosmic Rays

We close this tour of the CMB/particle intersection with possibly the oldest and most venerable connection between these two topics. Soon after the initial

discovery of the CMB, it was realized that cosmic rays with energy $E \gtrsim 5 \times 10^{19}$ eV can scatter from CMB photons and produce pions. If a cosmic ray is produced with an energy above 5×10^{19} eV, repeated scatterings will reduce its energy to below this threshold within a distance of about 50 Mpc (391–394) [the Greisen-Zatsepin-Kuzmin (GZK) bound]. These constraints have become increasingly intriguing recently, as several cosmic rays with energies $>10^{20}$ eV have been observed (395–398), and they do not appear to be coming from any identifiable astrophysical sources [e.g. radio galaxies or quasars (399)] as near as 50 Mpc (394, 397, 398, 400). So where are these cosmic rays coming from? Some possibilities are exotic production mechanisms such as topological defects (401–405), or supermassive unstable particles (406–408; see 409 for a review). If a recently claimed alignment of the highest-energy events with very distant radio quasars (410) is confirmed by larger numbers of events, then it may be that these cosmic rays are exotic particles that interact with baryons but not photons (411, 412), e.g. supersymmetric S_0 baryons (413–415). In the absence of any compelling traditional astrophysical origin, it seems that the simultaneous existence of the CMB and these cosmic rays may be pointing to some intriguing new particle physics.

8. SUMMARY, CURRENT RESULTS, AND FUTURE PROSPECTS

The primary cosmological observables pursued by CMB experiments are the frequency spectrum of the CMB, parameterized by μ and y distortions, and the angular temperature and polarization power spectra, $C_l^{\rm TT}$, $C_l^{\rm GG}$, $C_l^{\rm CC}$, $C_l^{\rm TG}$, $C_l^{\rm TC}$, and $C_l^{\rm GC}$. There are additional observables, such as higher-order correlation functions or cross-correlation of the CMB temperature/polarization with other diffuse extragalactic backgrounds. Rough estimates of the $C_l^{\rm TT}$ at degree angular scales were obtained (63) from the first generation of ground-based and balloon-borne CMB experiments. Forthcoming experiments will require far more sophisticated techniques for disentangling the CMB from foregrounds, and for recovering the power spectra from noisy data and from maps that cover only a fraction of the sky. A large literature is now devoted to these important issues, which we cannot review here.

Progress in CMB experiments is so rapid at the time of writing that any current data we might review would almost certainly become obsolete by the time of publication. We therefore refrain from showing any experimental results in detail and instead describe the current observations qualitatively. First, there is the isotropy of the CMB, which has long been explained only by inflation. Among the numerous pre-*COBE* models for the origin of large-scale structure, those based on a nearly scale-free spectrum of primordial adiabatic perturbations seem to account most easily for the amplitudes of both the large-angle CMB anisotropy measured by *COBE* and the amplitude of clustering in galaxy surveys. The galaxy distribution seems to be consistent with primordial Gaussianity.

Moreover, data from a large number of CMB experiments that probe the angular power spectrum at degree angular scales have now found (fairly convincingly) that there is significantly more power at degree angular separations ($l \sim 200$) than at *COBE* scales, as one would expect if the acoustic peaks do exist, but in apparent conflict with most theorists' expectations for the degree-scale anisotropy in topological-defect models. The existence of this small-scale anisotropy further suggests no more than a small level of reionization (i.e. $\tau \ll 1$). At the time of writing, the measurements are not precise enough to discern either the first or any higher peaks in the temperature power spectrum (some recent data are shown in Reference 416 and are usually updated at Reference 417). Some experiments have claimed to see the outline of a first acoustic peak at $l \sim 200$ (418) (which would indicate a flat Universe). Moreover, some maximum-likelihood analyses of combined results of all experiments claim that the data indicate a flat Universe (419, 420). However, these results are not yet robust.

Thus, although inflation is by no means yet in the clear, observations do seem to be pointing increasingly toward inflation. MAP and the Planck Surveyor will soon make far more precise tests of inflation (see 416 for simulated data from MAP and Planck). First of all, the predictions of primordial adiabatic perturbations will be tested with unprecedented precision by the peak structure in the CMB temperature power spectrum. If the peaks do appear, then MAP and the Planck Surveyor should be able to measure the total density Ω to a few percent or better (421) by determining the location of the first acoustic peak (178). Moreover, by fitting MAP and Planck satellite data to theoretical curves, such as those shown in Figure 3, precise information on the values of other classical cosmological parameters can also be obtained (150, 175, 194, 195, 422). If nonrelativistic matter outweighs baryons, then it should become evident with MAP and Planck. The existence of a cosmological constant will further be tested, and some of the tests of gravity, decaying particles, etc, that we have reviewed will become possible.

If MAP and Planck confirm that the Universe is flat and that structure grew from primordial adiabatic perturbations, then the next step will be to search for the gravitational-wave background predicted by inflation. Such a gravitational-wave background could be isolated uniquely with the curl component of the polarization. If the inflaton-potential height is $V^{1/4} \ll 10^{15}$ GeV, then the gravitational-wave background will be unobservably small. However, if inflation had something to do with grand unification (i.e. $V^{1/4} \sim 10^{15-16}$ GeV), as many theorists surmise, then the curl component of the polarization is conceivably detectable with the Planck Surveyor or with a realistic next-generation dedicated polarization satellite experiment. If detected, the curl component would provide a "smoking-gun" signature of inflation and indicate unambiguously that inflation occurred at $T \sim 10^{15-16}$ GeV. Although an observable signature is by no means guaranteed, even if inflation did occur, the prospects for peering directly back to 10^{-40} sec after the big bang are so tantalizing that a vigorous pursuit is certainly warranted.

ACKNOWLEDGMENTS

We thank R Caldwell, A Liddle, and L Wang for very useful comments. MK was supported by a DOE Outstanding Junior Investigator Award, DE-FG02-92ER40699, NASA Astrophysics Theory Program grant NAG5-3091, and the Alfred P. Sloan Foundation. AK was supported by NASA Astrophysics Theory Program grant NAG5-7015 and acknowledges the kind hospitality of the Institute for Advanced Study.

LITERATURE CITED

1. Alpher RA, Herman RC. *Phys. Rev.* 75:1089 (1949)
2. Gamow G. *Phys. Rev.* 70:572 (1946)
3. Penzias AA, Wilson RW. *Ap. J.* 142:419 (1965)
4. Dicke RH, Peebles PJE, Roll PG, Wilkinson DT. *Ap. J.* 142:414 (1965)
5. Corey BE, Wilkinson DT. *Bull. Am. Astron. Soc.* 8:351 (1976)
6. Smoot GF, Gorenstein MV, Muller RA. *Phys. Rev. Lett.* 39:898 (1977)
7. Smoot GF, et al. *Ap. J. Lett.* 371:L1 (1991)
8. Smoot GF, et al. *Ap. J. Lett.* 396:L1 (1992)
9. Kogut A, et al. *Ap. J.* 419:1 (1993)
10. Fixsen DJ, et al. *Ap. J.* 402:32 (1994)
11. Kneissl R, et al. *Astron. Astrophys.* 320:685 (1997)
12. Boughn SP, Crittenden RG, Turok NG. *New Astron.* 3:275 (1998)
13. Mather JC, et al. *Ap. J.* 420:439 (1994)
14. Wright EL, et al. *Ap. J.* 420:450 (1994)
15. Fixsen DJ, et al. *Ap. J.* 473:576 (1996)
16. Jones BJT, Wyse RFG. *Astron. Astrophys.* 149:144 (1976)
17. Kolb EW, Turner MS. *The Early Universe*. Redwood City, CA: Addison-Wesley (1990)
18. Peebles PJE. *Principles of Physical Cosmology*. Princeton, NJ: Princeton Univ. Press (1993)
19. Smoot GF, et al. *Ap. J.* 360:685 (1990)
20. Sachs RK, Wolfe AM. *Ap. J.* 147:73 (1967)
21. Guth AH, Pi S-Y. *Phys. Rev. Lett.* 49:1110 (1982)
22. Hawking SW. *Phys. Lett.* B115:29 (1982)
23. Linde AD. *Phys. Lett.* B116:335 (1982)
24. Starobinsky AA. *Phys. Lett.* B117:175 (1982)
25. Bardeen JM, Steinhardt PJ, Turner MS. *Phys. Rev. D* 46:645 (1983)
26. Wasserman I. *Phys. Rev. Lett.* 57:2234 (1986)
27. Hill CT, Schramm DN, Fry J. *Comments Nucl. Part. Phys.* 19:25 (1989)
28. Sahni V, Feldman HA, Stebbins A. *Ap. J.* 385:1 (1992)
29. Vilenkin A. *Phys. Rev. Lett.* 48:59 (1982)
30. Press WH. *Phys. Scripta* 21:702 (1980)
31. Zeldovich YaB, Kozbarev IY, Okun LB. *Zh. ETF* 67:3 (*Soviet Phys. JETP* 40:1) (1974)
32. Kibble TWB. *J. Phys.* A9:1387 (1976)
33. Zeldovich YaB. *MNRAS* 192:663 (1980)
34. Vilenkin A. *Phys. Rev. Lett.* 46:1169 (1981)
35. Silk J, Vilenkin A. *Phys. Rev. Lett.* 53:1700 (1984)
36. Turok N. *Phys. Rev. Lett.* 55:1801 (1985)
37. Press WH, Ryden BS, Spergel DN. *Ap. J.* 347:590 (1989)
38. Turok N. *Phys. Rev. Lett.* 24:2625 (1989)
39. Turok N. *Phys. Scripta* T36:135 (1991)
40. Barriola M, Vilenkin A. *Phys. Rev. Lett.* 63:341 (1989)
41. Bennett DP, Rhie SH. *Phys. Rev. Lett.* 65:1709 (1990)
42. Witten EW. *Nucl.Phys.* B246:557 (1985)
43. Witten EW, Thompson C, Ostriker JP. *Phys. Lett.* B180:231 (1986)

44. Seckel D, Turner MS. *Phys. Rev. D* 32:3178 (1985)
45. Turner MS, Wilczek F. *Phys. Rev. Lett.* 66:5 (1991)
46. Axenides M, Brandenberger R, Turner MS. *Phys. Lett.* B126:178 (1983)
47. Steinhardt PJ, Turner MS. *Phys. Lett.* B129:51 (1983)
48. Kofman LA, Linde AD. *Nucl. Phys.* B282:55 (1987)
49. Lyth DH. *Phys. Lett.* B236:408 (1990)
50. Linde AD. *Phys. Lett.* B259:38 (1991)
51. Kodama H, Sasaki M. *Int. J. Mod. Phys.* A1:265 (1986)
52. Efstathiou G, Bond JR. *MNRAS* 227:33 (1987)
53. Jaffe AH, Stebbins A, Frieman JA. *Ap. J.* 420:9 (1994)
54. Pen U-L, Seljak U, Turok N. *Phys. Rev. Lett.* 79:1611 (1997)
55. Albrecht A, Battye RA, Robinson J. *Phys. Rev. Lett.* 79:4736 (1997)
56. Allen B, et al. *Phys. Rev. Lett.* 79:2624 (1997)
57. Guth AH. *Phys. Rev. D* 28:347 (1981)
58. Linde AD. *Phys. Lett.* B108:389 (1982)
59. Albrecht A, Steinhardt PJ. *Phys. Rev. Lett.* 48:1220 (1982)
60. Lyth DH, Riotto A. hep-ph/9807278 (1998). *Phys. Rep.* In press (1999)
61. Liddle AR, Lyth DH. *Phys. Rep.* 231:1 (1993)
62. Lidsey JE, et al. *Rev. Mod. Phys.* 69:373 (1997)
63. White M, Scott D, Silk J. *ARAA* 32:319 (1994)
64. Hu W, White M. *New Astron.* 2:323 (1997)
65. Sunyaev RA, Zeldovich YaB. *ARAA* 18:537 (1980)
66. Rephaeli Y. *ARAA* 33:541 (1995)
67. Birkinshaw M. *Phys. Rep.* 310:97 (1999)
68. Danese L, De Zotti G. *Riv. Nuovo Cimiento* 7:277 (1977)
69. Lightman AP. *Ap. J.* 244:392 (1981)
70. Danese L, De Zotti G. *Astron. Astrophys.* 107:39 (1982)
71. Sarkar S, Cooper AM. *Phys. Lett.* B148:347 (1983)
72. Fukugita M, Kawasaki M. *Ap. J.* 353:384 (1990)
73. Burigana C, Danese L, De Zotti G. *Astron. Astrophys.* 246:49 (1991)
74. Burigana C, Danese L, De Zotti G. *Ap. J.* 379:1 (1991)
75. Hu W, Silk J. *Phys. Rev. D* 48:485 (1993)
76. Shafer RA, et al. *Bull. Am. Astron. Soc.* 187:71.10 (1995)
77. http://map.gsfc.nasa.gov
78. http://astro.estec.esa.nl/SA-general/Projects/Planck/
79. Kamionkowski M, Kosowsky A, Stebbins A. *Phys. Rev. Lett.* 78:2058 (1997)
80. Kamionkowski M, Kosowsky A, Stebbins A. *Phys. Rev. D* 55:7368 (1997)
81. Seljak U, Zadarriaga M. *Phys. Rev. Lett.* 78:2054 (1997)
82. Zaldarriaga M, Seljak U. *Phys. Rev. D* 55:1830 (1997)
83. Stebbins A. astro-ph/9609149 (1996)
84. Scaramella R, Vittorio N. *Ap. J.* 375:439 (1991)
85. Luo X, Schramm DN. *Phys. Rev. Lett.* 71:1124 (1993)
86. Luo X. *Ap. J. Lett.* 427:L71 (1994)
87. Ferreira PG, Magueijo J, Silk J. *Phys. Rev. D* 56:4592 (1997)
88. Coles P. *MNRAS* 234:509 (1988)
89. Gott JR, et al. *Ap. J.* 352:1 (1990)
90. Kogut A, et al. *Ap. J. Lett.* 464:L29 (1996)
91. Winitzki S, Kosowsky A. *New Astron.* 3:75 (1997)
92. Schmalzing J, Gorski KM. *MNRAS* 297: 355 (1998)
93. Bond JR, Efstathiou G. *MNRAS* 226:655 (1987)
94. Vittorio N, Juskiewicz R. *Ap. J.* 314:L29 (1987)
95. Ferreira PG, Magueijo J. *Phys. Rev. D* 55:3358 (1997)
96. Lewin A, Albrecht A, Magueijo J. *MNRAS Lett.* 302:L131 (1999)
97. Pando J, Valls-Gabaud D, Fang LZ. *Phys. Rev. Lett.* 81:4568 (1998)

98. Hobson MP, Jones AW, Lasenby AN. astro-ph/9810200 (1998)
99. Knox L, Turner MS. *Phys. Rev. Lett.* 70:371 (1993)
100. Freese K, Frieman JA, Olinto AV. *Phys. Rev. Lett.* 65:3233 (1990)
101. Adams FC, Bond JR, Freese K, Frieman JA, Olinto AV. *Phys. Rev. D* 47:426 (1993)
102. Randall L, Soljacic M, Guth AH. *Nucl. Phys.* B472:377 (1996)
103. Lyth DH, Stewart E. *Phys. Lett.* B252:336 (1990)
104. Kamionkowski M, Spergel DN. *Ap. J.* 432:7 (1994)
105. Gott JR. *Nature* 295:304 (1982)
106. Bucher M, Goldhaber AS, Turok N. *Phys. Rev. D* 52:3314 (1995)
107. Ratra B, Peebles PJE. *Phys. Rev. D* 52:1837 (1995)
108. Linde AD. *Phys. Lett.* B351:99 (1995)
109. Cornish NJ, Spergel DN, Starkman GD. *Phys. Rev. Lett.* 77:215 (1996)
110. Hawking SW, Turok N. *Phys. Lett.* B425:25 (1998)
111. Linde AD. *Particle Physics and Inflationary Cosmology*. New York: Harwood Academic (1990)
112. Abbott LF, Wise M. *Nucl. Phys.* B244:541 (1984)
113. Peebles PJE, Yu JT. *Ap. J.* 162:815 (1970)
114. Harrison ER. *Phys. Rev. D* 1:2726 (1970)
115. Zeldovich YaB. *MNRAS* 160:1P (1972)
116. Birrell ND. Davies PCW. *Quantum Fields in Curved Spacetime*. Cambridge, UK: Cambridge Univ. Press (1982)
117. Starobinsky AA. *Sov. Astron. Lett.* 11:133 (1985)
118. Liddle AR, Lyth DH. *Phys. Lett.* B291:391 (1992)
119. Davis RL, et al. *Phys. Rev. Lett.* 69:1856 (1992)
120. Lucchin F, Matarrese S, Mollerach S. *Ap. J. Lell.* 401:L49 (1992)
121. Lidsey JE, Coles P. *MNRAS Lett.* 258:L57 (1992)
122. Turner MS. *Phys. Rev. D* 48:3502 (1993)
123. Turner MS. *Phys. Rev. D* 48:5539 (1993)
124. Copeland EJ, Kolb EW, Liddle AR Lidsey JE. *Phys. Rev. Lett.* 71:219 (1993)
125. Copeland EJ, Kolb EW, Liddle AR Lidsey JE. *Phys. Rev. D* 48:2529 (1993)
126. Copeland EJ, Kolb EW, Liddle AR Lidsey JE. *Phys. Rev. D* 49:1840 (1994)
127. Liddle AR, Turner MS. *Phys. Rev. D* 50:758 (1994)
128. Kosowsky A, Turner MS. *Phys. Rev. D* 52:1739 (1995)
129. Mollerach S, Matarrese S, Lucchin F. *Phys. Rev. D* 50:4835 (1994)
130. Zibin JP, Scott D, White M. astro-ph/9901028 (1999)
131. Bennett CL, et al. *Ap. J. Lett.* 464:L1 (1996)
132. Mukhanov V, Zelnikov M. *Nucl. Phys.* B263:160 (1991)
133. Polarski D, Starobinsky AA. *Nucl. Phys.* B385:623 (1992)
134. Peter P, Polarski D, Starobinsky AA. *Phys. Rev. D* 50:4827 (1994)
135. Starobinsky AA, Yokoyama J. gr-qc/9502002 (1995)
136. Garcia-Bellido J, Wands D. *Phys. Rev. D* 53:5437 (1996)
137. Sasaki M, Stewart E. *Prog. Theor. Phys.* 95:71 (1996)
138. Kawasaki M, Sugiyama N, Yanagida T. *Phys. Rev. D* 54:2442 (1996)
139. Linde A, Mukhanov V. *Phys. Rev. D* 56:535 (1997)
140. Mukhanov VF, Steinhardt, PJ. *Phys. Lett.* B422:52 (1998)
141. Kanazawa T, et al. *Prog. Theor. Phys.* 100:1055 (1998)
142. Kanazawa T, et al. astro-ph/9805102 (1998)
143. Allen TJ, Grinstein B, Wise M. *Phys. Lett.* 197B:66 (1987)
144. Salopek DS, Bond JR, Bardeen JM. *Phys. Rev. D* 40:1753 (1989)
145. Falk T, Rangarajan R, Srednicki M. *Ap. J. Lett.* 403:L1 (1993)
146. Gangui A, Lucchin F, Matarrese S,

Mollerach S. *Ap. J.* 430:447 (1994)
147. Gangui A. *Phys. Rev. D* 50:3684 (1994)
148. Ferreira PG, Magueijo J, Gorski KM. *Ap. J. Lett.* 503:L1 (1998)
149. Peebles PJE. *Large-Scale Structure of the Universe*. Princeton, NJ: Princeton Univ. Press (1980)
150. Kinney W, Dodelson S, Kolb EW. *Phys. Rev. D* 56:3207 (1998)
151. Kinney W. *Phys. Rev. D* 58:123506 (1998)
152. Hu W, Sugiyama N. *Phys. Rev. D* 50:627 (1994)
153. Kofman L, Starobinsky A. *Sov. Astron. Lett.* 11:271 (1986)
154. Bardeen JM. *Phys. Rev. D* 22:1882 (1980)
155. Kodama H, Sasaki M. *Prog. Theor. Phys. Suppl.* 78:1 (1984)
156. Mukhanov VF, Feldman HA, Brandenberger RH. *Phys. Rep.* 215:203 (1992)
157. Ma C-P, Bertschinger E. *Ap. J.* 455:7 (1995)
158. Hu W, Scott D, Sugiyama N, White M. *Phys. Rev. D* 52:5498 (1995)
159. Seljak U, Zaldarriaga M. *Ap. J.* 469:437 (1996)
160. Wilson ML, Silk J. *Phys. Scripta* 21:708 (1980)
161. Wilson ML, Silk J. *Ap. J.* 243:14 (1981)
162. Silk J, Wilson ML. *Ap. J. Lett.* 244:L37 (1981)
163. Bond JR, Efstathiou G. *Ap. J. Lett.* 285:L45 (1984)
164. Vittorio N, Silk J. *Ap. J.* 285:L39 (1984)
165. Holtzman JA. *Ap. J. Suppl.* 71:1 (1989)
166. Milaneschi E, Valdarnini R. *Astron. Astrophys.* 162:5 (1986)
167. Harari D, Zaldarriaga M. *Phys. Lett.* B319:96 (1993)
168. Crittenden RG, Davis RL, Steinhardt PJ. *Ap. J. Lett.* 417:L13 (1993)
169. Frewin RA, Polnarev AG, Coles P. *MNRAS Lett.* 266:L21 (1994)
170. Ng KL, Ng KW. *Ap. J.* 445:521 (1995)
171. Kosowsky A. *Ann. Phys.* 246:49 (1996)
172. Hu W, White M. *Phys. Rev. D* 56:596 (1997)
173. Bertschinger E. astro-ph/9506070 (1995)
174. Hu W, Sugiyama N. *Ap. J.* 471:542 (1996)
175. Jungman G, Kamionkowski M, Kosowsky A, Spergel DN. *Phys. Rev. D* 54: 1332 (1996)
176. Sakharov AD. *JETP* 49:345 (1965) [*Sov. Phys. JETP* 22:241 (1966)]
177. Sunyaev RA, Zeldovich YaB. *Astrophys. Sp. Sci.* 7:3 (1970)
178. Kamionkowski M, Spergel DN, Sugiyama N. *Ap. J. Lett.* 426:L57 (1994)
179. Tegmark M, Silk J, Blanchard A. *Ap. J.* 420:484 (1994)
180. Haiman Z, Loeb A. *Ap. J.* 483:21 (1997)
181. Crittenden RG, Turok NG. *Phys. Rev. Lett.* 76:575 (1996)
182. Kamionkowski M. *Phys. Rev. D* 54:4169 (1996)
183. Kinkhabwala A, Kamionkowski M. astro-ph/9808320 (1998)
184. Zaldarriaga M, Seljak U. astro-ph/ 9810257 (1998)
185. Hu W, Sugiyama N. *Phys. Rev. D* 51:2599 (1995)
186. Hu W, White M. *Phys. Rev. Lett.* 77:1687 (1996)
187. Kosowsky A. astro-ph/9811163 (1998)
188. Hu W, White M. *Ap. J.* 471:30 (1996)
189. Zaldarriaga M, Harari DD. *Phys. Rev. D* 52:3276 (1995)
190. Zaldarriaga M, Spergel DN. *Phys. Rev. Lett.* 79:2180 (1997)
191. Kamionkowski M, Kosowsky A. *Phys. Rev. D* 67:685 (1998)
192. Zaldarriaga M. *Phys. Rev. D* 55:1822 (1997)
193. Knox L. *Phys. Rev. D* 52:4307 (1995)
194. Bond JR, Efstathiou G, Tegmark M. *MNRAS Lett.* 291:L33 (1997)
195. Zaldarriaga M, Seljak U, Spergel DN. *Ap. J.* 488:1 (1997)
196. Copeland EJ, Grivell IJ, Liddle AR. *MNRAS* 298:1233 (1998)
197. Goldberg DM, Spergel DN. astro-ph/ 9811251 (1998)
198. Kamionkowski M, Jaffe AH. *Nature* 395:639 (1998)

199. Hindmarsh M, Kibble TWB. *Rep. Prog. Phys.* 58:47 (1995)
200. Vilenkin A. *Phys. Rep.* 121:263 (1985)
201. Vilenkin A, Shellard EPS. *Cosmic Strings and Other Topological Defects*. Cambridge, UK: Cambridge Univ. Press (1994)
202. Stebbins A, Turner MS. *Ap. J. Lett.* 339:L13 (1989)
203. Turner MS, Watkins R, Widrow L. *Ap. J. Lett.* 367:L43 (1991)
204. Turok N, Spergel DN. *Phys. Rev. Lett.* 66:3093 (1991)
205. Jaffe A. *Phys. Rev. D* 49:3893 (1994)
206. Kamionkowski M, March-Russell J. *Phys. Rev. Lett.* 69:1485 (1992)
207. Holman R, et al. *Phys. Rev. Lett.* 69:1489 (1992)
208. Albrecht A, Coulson D, Ferreira PG, Magueijo J. *Phys. Rev. Lett.* 76:1413 (1996)
209. Magueijo J, Albrecht A, Coulson D, Ferreira P. *Phys. Rev. D* 54:3727 (1996)
210. Hu W, White M. *Phys. Rev. D* 55:3288 (1997)
211. Stebbins A, Veeraraghavan S. *Ap. J.* 365:37 (1990)
212. Turok N. *Phys. Rev. D* 54:3686 (1996)
213. Turok N. *Phys. Rev. Lett.* 77:4138 (1996)
214. Hu W, Spergel DN, White M. *Phys. Rev. D* 55:3288 (1997)
215. Durrer R, Kunz M. *Phys. Rev. D* 57:R3199 (1998)
216. Durrer R, Sakellariadou M. *Phys. Rev. D* 56:4480 (1997)
217. Seljak U, Pen U, Turok N. *Phys. Rev. Lett.* 79:1615 (997)
218. Crittenden RG, Turok NG. *Phys. Rev. Lett.* 75:2642 (1995)
219. Durrer R, Gangui A, Sakellariadou M. *Phys. Rev. Lett.* 76:579 (1996)
220. Durrer R, Zhou ZH. *Phys. Rev. D* 53:5394 (1996)
221. Contaldi C, Hindmarsh M, Magueijo J. *Phys. Rev. Lett.* 82:679 (1999)
222. Albrecht A, Battye RA, Robinson J. *Phys. Rev. Lett.* 80:4847 (1998)
223. Albrecht A, Battye RA, Robinson J. astro-ph/9711121 (1997)
224. Hu W. *Phys. Rev. D* 59:021301 (1999)
225. Magueijo J, Albrecht A, Coulson D, Ferreira P. *Phys. Rev. Lett.* 76:2617 (1996)
226. Pen U-L. astro-ph/9804083 (1998)
227. Jeannerot R. *Phys. Rev. D* 53:5426 (1996)
228. Linde A, Riotto A. *Phys. Rev. D* 56:1841 (1997)
229. Avelino PP, Caldwell RR, Martins CJAP. astro-ph/9809130 (1998)
230. Scherrer R, Bertschinger E. *Ap. J.* 381:349 (1991)
231. Perivolaropoulos L. *Phys. Rev. D* 48:1530 (1993)
232. Bennett D, Rhie SH. *Ap. J. Lett.* 406:L7 (1993)
233. Gilbert AM, Perivolaropoulos L. *Astropart. Phys.* 3:283 (1995)
234. Scherrer RJ, Schaefer RK. *Ap. J.* 446:44 (1995)
235. Kaiser N, Stebbins A. *Nature* 310:391 (1984)
236. Moessner R, Perivolaropoulos L, Brandenberger R. *Ap. J.* 425:365 (1994)
237. Perivolaropoulos L. astro-ph/9704011 (1997)
238. Perivolaropoulos L. *Phys. Rev. Lett. D* 58:103507 (1998)
239. Turok N, Spergel DN. *Phys. Rev. Lett.* 64:2736 (1990)
240. Turok N. *Ap. J. Lett.* 473:L5 (1996)
241. Perlmutter S, et al. *Ap. J.* 483:565 (1997)
242. Perlmutter S, et al. astro-ph/9812133. *Ap. J.* In press (1999)
243. Riess AG, et al. Astron. J. 116:1009 (1998)
244. Athanassopoulos C, et al. *Phys. Rev. Lett.* 75:2650 (1995)
245. Athanassopoulos C, et al. *Phys. Rev. C* 54:2685 (1995)
246. Jungman G, Kamionkowski M, Griest K. *Phys. Rep.* 267:195 (1996)
247. Turner MS. *Phys. Rep.* 197:67 (1990)
248. Raffelt GG. *Phys. Rep.* 198:1 (1990)

249. White SDM, Navarro JF, Evrard AE, Frenk CS. *Nature* 366:429 (1993)
250. Tyson JA, Kochanski GP, Dell'Antonio IP. *Ap. J. Lett.* 498:L107 (1998)
251. Shafi Q, Stecker FW. *Phys. Rev. Lett.* 53:1292 (1984)
252. van Dalen A, Schaefer RK. *Ap. J.* 398:33 (1992)
253. Davis M, Summers F, Schlegel D. *Nature* 359:393 (1992)
254. Klypin A, Holtzman J, Primack J, Regos E. *Ap. J.* 416:1 (1993)
255. Primack JR, et al. *Phys. Rev. Lett.* 74:2160 (1995)
256. Bonometto SA, Pierpaoli E. *New Astron.* 3:6 (1998)
257. Dodelson S, Gates E, Stebbins A. *Ap. J.* 467:10 (1996)
258. Lopez RE, Dodelson S, Heckler A, Turner MS. astro-ph/9803095 (1998)
259. Hu W, Eisenstein DJ, Tegmark M. *Phys. Rev. Lett.* 80:5255 (1998)
260. Steigman G, Schramm DN, Gunn JE. *Phys. Lett.* B66:202 (1977)
261. Copi CJ, Schramm DN, Turner MS. *Phys. Rev. D* 55:3389 (1997)
262. Carroll SM, Press WH, Turner EL. *ARAA*30:499 (1992)
263. Efstathiou G, et al. astro-ph/9812226 (1998)
264. Garnavich PM, et al. *Ap. J.* 509:74 (1998)
265. Tegmark M. astro-ph/9809201 (1998)
266. Tegmark M, Eisenstein DJ, Hu W. astro-ph/9804168 (1998)
267. White M. *Ap. J.* 506:495 (1998)
268. Lineweaver CH. *Ap. J. Lett.* 505:L69 (1998)
269. Ratra B, Peebles PJE. *Phys. Rev. D* 27:3406 (1988)
270. Sugiyama N, Sato K. *Ap. J.* 387:439 (1992)
271. Frieman JA, Hill CT, Stebbins A, Waga I. *Phys. Rev. Lett.* 75:2077 (1995)
272. Coble K, Dodelson S, Frieman J. *Phys. Rev. D* 55:1851 (1997)
273. Silviera V, Waga I. *Phys. Rev. D* 56:4625 (1997)
274. Turner MS, White M. *Phys. Rev. D* 56:4439 (1997)
275. Chiba T, Sugiyama N, Nakamura T. *MNRAS Lett.* 289:L5 (1997)
276. Caldwell RR, Dave R, Steinhardt PJ. *Phys. Rev. Lett.* 80:1582 (1998)
277. Chiba T, Sugiyama N, Nakamura T. *MNRAS* 301:72 (1998)
278. Lucchin F, Matarrese S. *Phys. Rev. D* 32:1316 (1985)
279. Wetterich C. *Nulc. Phys.* B302:668 (1988)
280. Wands D, Copeland EJ, Liddle AR. *Ann. NY Acad. Sci.* 688:647 (1993)
281. Ferreira PG, Joyce M. *Phys. Rev. Lett.* 79:4740 (1997)
282. Copeland EJ, Liddle AR, Wands D. *Phys. Rev. D* 57:4686 (1998)
283. Liddle AR, Scherrer RJ. *Phys. Rev. D* 59:023509 (1999)
284. Zlatev I, Wang L, Steinhardt PJ. *Phys. Rev. Lett.* 82:896 (1999)
285. Steinhardt PJ, Wang L, Zlatev I. astro-ph/9812313 (1998)
286. Huey G, et al. *Phys. Rev. D* 59:063005 (1999)
287. Hu W, Eisenstein DJ, Tegmark M, White M. *Phys. Rev. D* 59:023512 (1999)
288. Wang L, et al. astro-ph/9901388 (1999)
289. Hu W, Silk J. *Phys. Rev. Lett.* 70:2661 (1993)
290. Ellis J, et al. *Nucl. Phys.* B373:399 (1992)
291. Lopez RE, Dodelson S, Scherrer RJ, Turner MS. *Phys. Rev. Lett.* 81:3075 (1998)
292. Hannestad S. *Phys. Lett.* B431:363 (1998)
293. Hannestad S. *Phys. Rev. Lett.* 80:4621 (1998)
294. Varshalovich DA, Potekhin AY. *Space Sci. Rev.* 74:259 (1995)
295. Marciano W. *Phys. Rev. Lett.* 52:489 (1984)
296. Barrow JD. *Phys. Rev. D* 35:1805 (1987)
297. Damour T, Polyakov AM. *Nulc. Phys.* B423:532 (1994)
298. Carroll SM. *Phys. Rev. Lett.* 81:3067 (1998)

299. Shylakhter AI. *Nature* 264:340 (1976)
300. Damour T, Dyson F. *Nucl. Phys.* B480:37 (1996)
301. Savedoff MP. *Nature* 178:688 (1956)
302. Drinkwater MJ, Webb JK, Barrow JD, Flambaum VV. *MNRAS* 298:457 (1998)
303. Cowie LL, Songaila A. *Ap. J.* 453:596 (1995)
304. Ivanchik AV, Potekhin AY, Varshalovich DA. *Astron. Astrophys.* 343:439 (1999)
305. Webb JK, et al. *Phys. Rev. Lett.* 82:884 (1999)
306. Kolb EW, Perry MJ, Walker TP. *Phys. Rev. D* 33:869 (1986)
307. Kaplinghat M, Scherrer RJ, Turner MS. astro-ph/9810133 (1998)
308. Hannestad S. astro-ph/9810102 (1998)
309. Lachieze-Rey M, Luminet JP. *Phys. Rep.* 254:135 (1995)
310. Zeldovich YaB, Starobinsky AA. *Soviet Astron. Lett.* 10:135 (1984)
311. Gott JR. *MNRAS* 193:153 (1980)
312. Ellis GFR, Schreiber G. *Mod. Phys. Lett.* A115:97 (1986)
313. Fang LZ, Mo H. *Mod. Phys. Lett.* A2:229 (1987)
314. Sokolov IY. *JETP Lett.* 57:617 (1993)
315. Starobinsky AA. *JETP Lett.* 57:622 (1993)
316. Fang LZ. *Mod. Phys. Lett.* A8:2615 (1993)
317. Stevens D, Scott D, Silk J. *Phys. Rev. Lett.* 71:20 (1993)
318. Jing YP, Fang LZ. *Phys. Rev. Lett.* 73:1882 (1994)
319. de Oliveira-Costa A, Smoot GF. *Ap. J.* 448:477 (1995)
320. de Oliveira-Costa A, Smoot GF, Starobinsky AA. *Ap. J.* 468:457 (1996)
321. Scannapieco E, Levin J, Silk J. astro-ph/9811226 (1998)
322. Levin J, Scannapieco E, Silk J. *Phys. Rev. D* 58:103516 (1998)
323. Cornish NJ, Spergel DN, Starkman GD. *Phys. Rev. D* 57:5982 (1998)
324. Cornish NJ, Spergel DN, Starkman GD. *Proc. Nat. Acad. Sci.* 95:82 (1998)
325. Weeks JR. *Class. Quant. Grav.* 15:2599 (1998)
326. Levin J, et al. *Phys. Rev. D* 58:123006 (1998)
327. Levin JJ, Barrow JD, Bunn EF, Silk J. *Phys. Rev. Lett.* 79:974 (1997)
328. Souradeep T, Pogosyan D, Bond JR. *Proc. XXXIII Recontres de Moriond, Jan. 17–24, 1998, Les Arc, France* (1998)
329. Turner MS, Widrow LM. *Phys. Rev. D* 37:2743 (1988)
330. Carroll SM, Field GB. *Phys. Rev. D* 43:3789 (1991)
331. Garretson WD, Field GB, Carroll SM. *Phys. Rev. D* 46:5346 (1992)
332. Ratra B. *Ap. J. Lett.* 391:L1 (1992)
333. Dolgov AD. *Phys. Rev. D* 48:2499 (1993)
334. Gasperini M, Giovannini M, Veneziano G. *Phys. Rev. Lett.* 75:3796 (1995)
335. Gasperini M, Giovannini M, Veneziano G. *Phys. Rev. D* 52:6651 (1995)
336. Vachaspati T. *Phys. Lett.* B265:258 (1991)
337. Enqvist K, Olesen P. *Phys. Lett.* B319:178 (1993)
338. Quashnock J, Loeb A, Spergel DN. *Ap. J. Lett.* 344:L49 (1989)
339. Cheng B, Olinto A. *Phys. Rev. D* 50:2421 (1994)
340. Enqvist K, Olensen P. *Phys. Lett.* B329:195 (1994)
341. Dolgov AD, Silk J. *Phys. Rev. D* 47:3144 (1993)
342. Giovannini M. *Phys. Rev. D* 56:3198 (1997)
343. Kosowsky A, Loeb A. *Ap. J.* 469:1 (1996)
344. Harari DD, Hayward J, Zaldarriaga M. *Phys. Rev. D* 55:1841 (1996)
345. Adams J, Danielsson UH, Grasso D, Rubinstein H. *Phys. Lett.* B388:253 (1996)
346. Durrer R, Kahniashvili T, Yates A. *Phys. Rev. D* 58:123004 (1998)
347. Subramanian K, Barrow JD. *Phys. Rev. Lett.* 81:3575 (1998)
348. Scannapieco ES, Ferreira PG. *Phys. Rev. D* 56:4578 (1997)

349. Barrow JD, Ferreira PG, Silk J. *Phys. Rev. Lett.* 78:3610 (1997)
350. Novikov ID. *Soviet Astron.* 12:427 (1968)
351. Barrow JD, Juskiewicz R, Sonoda DH. *MNRAS* 213:917 (1985)
352. Lee TD, Yang CN. *Phys. Rev.* 104:254 (1956)
353. Wu CS, et al. *Phys. Rev.* 105:1413 (1957)
354. Lue A, Wang L, Kamionkowski M. astro-ph/9812088 (1998)
355. Lepora N. gr-qc/9812077 (1998)
356. Carroll SM, Field GB. *Phys. Rev. D* 41:1231 (1990)
357. Stecker, FW. *Ann. NY Acad. Sci.* 375:69 (1981)
358. Kinney WH, Kolb EW, Turner MS. *Phys. Rev. Lett.* 79:2620 (1997)
359. Cohen AG, DeRujula A, Glashow SL. *Ap. J.* 495:539 (1998)
360. Bergmann PG. *Int. J. Theor. Phys.* 1:25 (1968)
361. Nordtvedt K. *Ap. J.* 161:1059 (1970)
362. Wagoner RV. *Phys. Rev. D* 1:3209 (1970)
363. Bekenstein JD. *Phys. Rev. D* 15:1458 (1977)
364. Bekenstein JD, Meisels A. *Phys. Rev. D* 18:4378 (1978)
365. Jordan P. *Nature* 164:367 (1949)
366. Jordan P. *Z. Phys.* 157:112 (1955)
367. Fierz M. *Helv. Phys. Acta* 19:128 (1956)
368. Brans C, Dicke RH. *Phys. Rev.* 124:925 (1961)
369. Dicke RH. *Phys. Rev.* 125:2163 (1962)
370. Dicke RH. *Phys. Rev.* 152:1 (1968)
371. La D, Steinhardt PJ. *Phys. Rev. Lett.* 62:376 (1989)
372. La D, Steinhardt PJ. *Phys. Lett.* B220:375 (1989)
373. Weinberg EJ. *Phys. Rev. D* 40:3950 (1989)
374. La D, Steinhardt PJ, Bertschinger EW. *Phys. Lett.* B220:375 (1989)
375. Steinhardt PJ, Accetta FS. *Phys. Rev. Lett.* 64:2740 (1990)
376. Barrow JD, Maeda K. *Nucl. Phys.* B341:294 (1990)
377. Garcia-Bellido J, Quiros M. *Phys. Lett.* B243:45 (1990)
378. Holman R, Kolb EW, Wang Y. *Phys. Rev. Lett.* 65:17 (1990)
379. Will CM. *Theory and Experiment in General Relativity* Cambridge, UK: Cambridge Univ. Press (1993)
380. Will CM. gr-qc/9811036 (1998)
381. Damour T, Nordtvedt. *Phys. Rev. Lett.* 70:2217 (1993)
382. Damour T, Nordtvedt. *Phys. Rev. D* 48:3436 (1993)
383. Liddle AR, Mazumdar A, Barrow JD. *Phys. Rev. D* 58:027302 (1998)
384. Nariai H. *Prog. Theor. Phys.* 42:544 (1969)
385. Baptista JP, Fabris JC, Goncalves SVB. gr-qc/9603015 (1996)
386. Chiba T, Sugiyama N, Yokoyama J. *Nucl. Phys.* B530:304 (1998)
387. Kamionkowski M, Turner MS. *Phys. Rev. D* 42:3310 (1990)
388. Damour T, Gunlach C. *Phys. Rev. D* 43:3873 (1991)
389. Casa JA, Garcia-Bellido J, Quiros M. *Mod. Phys. Lett.* A7:447 (1992)
390. Damour T, Pichon B. astro-ph/9807176 (1998)
391. Greisen K. *Phys. Rev. Lett.* 16:748 (1966)
392. Zatsepin GT, Kuzmin VA. *JETP Lett.* 4:78 (1966)
393. Cronin JW. *Nucl. Phys. Proc. Suppl.* 28B:234 (1992)
394. Elbert J, Sommers P. *Ap. J.* 441:151 (1995)
395. Linsley J. *Phys. Rev. Lett.* 10:146 (1963)
396. Bird DJ, et al. *Ap. J.* 424:491 (1994)
397. Hayashida N, et al. *Phys. Rev. Lett.* 73:3491 (1994)
398. Bird DJ, et al. *Ap. J.* 441:144 (1995)
399. Hillas AM. *ARAA*22:425 (1984)
400. Biermann P. *J. Phys.* G23:1 (1997)
401. Hill C, et al. *Phys. Rev. D* 34:1622 (1986)
402. Aharonian FA, Bhattacharjee P, Schramm DN. *Phys. Rev. D* 46:4188 (1992)

403. Bhattacharjee P, Hill CT, Schramm DN. *Phys. Rev. Lett.* 69:567 (1992)
404. Chi X, Dahanayake C, Wdowczyk J, Wolfendale AW. *Astropart. Phys.* 1:239 (1993)
405. Sigl G, Schramm DN, Bhattacharjee P. *Astropart. Phys.* 2:401 (1994)
406. Kuzmin VA, Rubakov VA. *Phys. Atom. Nucl.* 61:1028 (1998)
407. Berezinsky V, Kachelreiss M. *Phys. Lett.* B434:61 (1998)
408. Birkel M, Sarkar S. *Astropart. Phys.* 9:297 (1998)
409. Bhattacharjee P, Sigl G. astro-ph/9811011 (1998)
410. Farrar GR, Biermann PL. *Phys. Rev. Lett.* 81:3579 (1998)
411. Chung DJH, Farrar GR, Kolb EW. *Phys. Rev. D* 57:4606 (1998)
412. Albuquerque IFM, Farrar GR, Kolb EW. *Phys. Rev. D* 59:015021 (1999)
413. Farrar GR. *Phys. Rev. Lett.* 53:1029 (1984)
414. Farrar GR. *Phys. Rev. D* 51:3904 (1995)
415. Farrar GR. *Phys. Rev. Lett.* 76:4111 (1996)
416. Kamionkowski M. *Science* 280:1397 (1998)
417. Tegmark M. http://www.sns.ias.edu/max/experiments.html (1999)
418. Peterson J. private communication (1999)
419. Lineweaver CH, Barbosa D. *Ap. J.* 496:624 (1998)
420. Hancock S, et al. *MNRAS Lett.* 29:L1 (1998)
421. Jungman G, Kamionkowski M, Kosowsky A, Spergel DN. *Phys. Rev. Lett.* 76:1007 (1996)
422. Bond JR, Efstathiou G. astro-ph/9807103 (1998)

Annual Review of Nuclear and Particle Science
Volume 49, 1999

CONTENTS